Photon Opacities in Highly-Magnetized Neutron Star Magnetospheres

Kun Hu (Rice U)
Matthew G. Baring (Rice U)
Zorawar Wadiasingh (GSFC)
Alice K. Harding (GSFC)

06/12/2019 @ GSFC

Magnetars

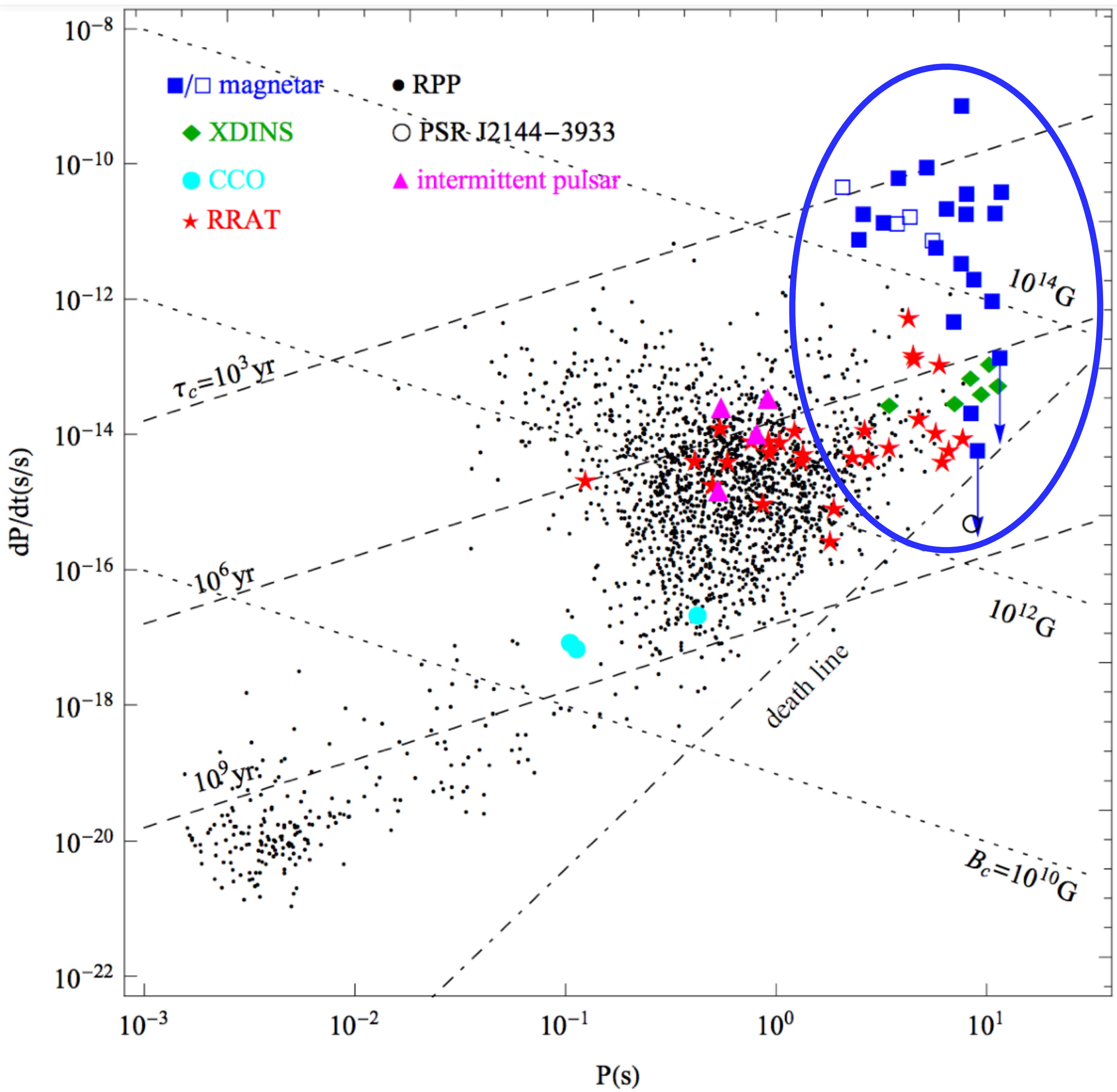

Figure from Zhou et al. 2015

- long spin periods ~2-12s and high spin down rates
- high inferred magnetic fields > 10^{13} G

$$B_p \sim 6.4 \times 10^{19} \sqrt{P\dot{P}} \quad \mathrm{G}$$

- persistent X-ray emission
- sporadic bursting activities

Persistent Emission

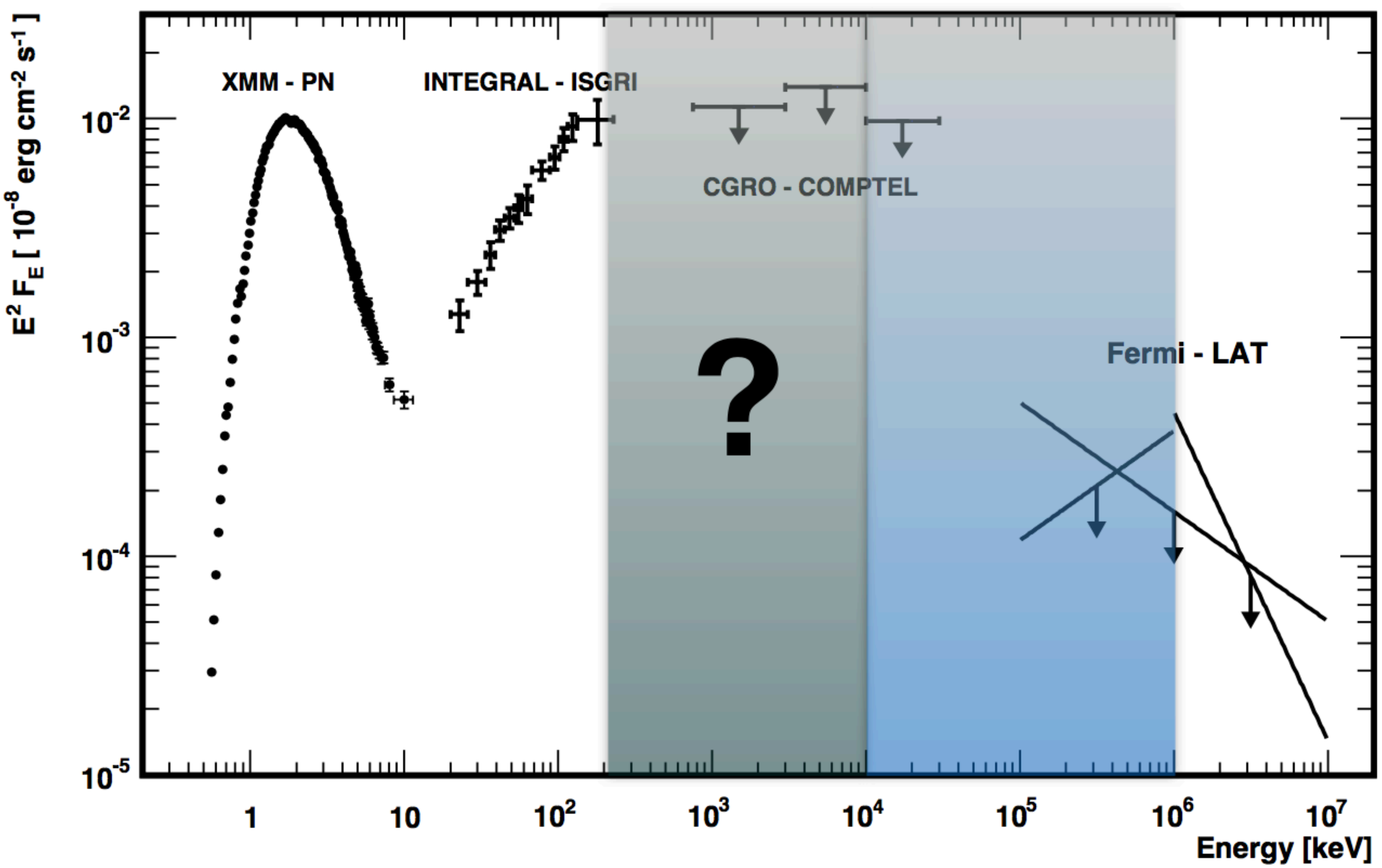

Total spectra of 4U 0142+61 as measured with different instruments. Figure adapted from Abdo et al. (2010)

- in quiescent state, magnetars emit bright X-ray with luminosities (10^{34}-10^{36} erg/s) exceeding spin down energy loss
- soft X-ray (<10 keV) spectra : Thermal + PL
- hard X-ray (>10 keV) spectra : Flat PL
- spectral turnover at a few hundred keV

Resonant inverse Compton scattering

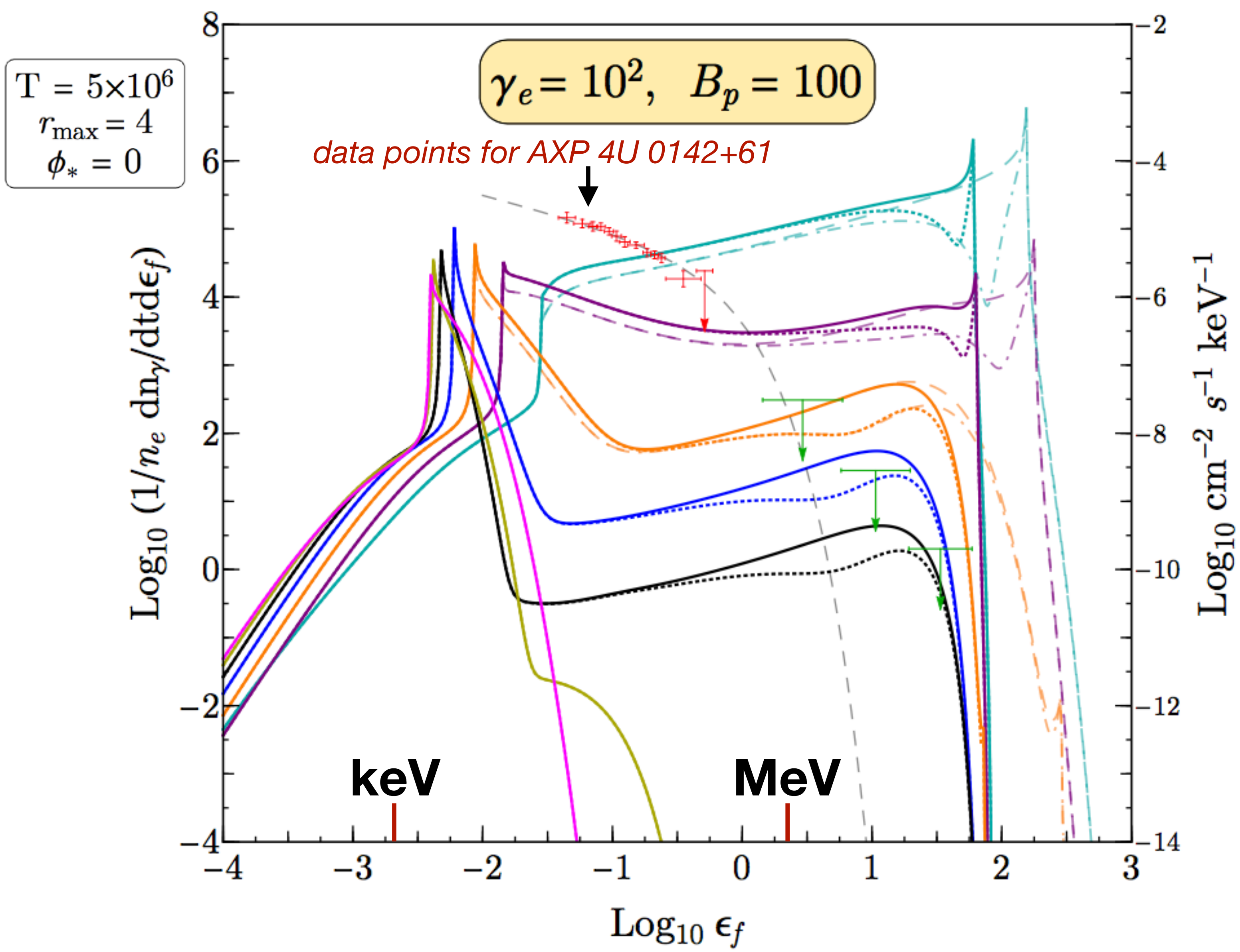

Wadiasingh et al. (2018)

- non-thermal hard X-ray persistent emission: resonant inverse Compton scattering
- electrons are accelerated along closed field lines
- currents/charge densities along closed field lines far exceed Goldreich-Julian values.
- extremely efficient due to the predominance of scatterings in the fundamental cyclotron resonance

Flaring Activities

- Short Bursts

  peak luminosity ~10^{37}-10^{43} erg/s, last ~ 0.1s

- Intermediate flares

  lasting ~1-40 s , peak luminosity ~10^{41}-10^{43} erg/s

- Giant Flares

  lasting~0.2 s, peak luminosity~10^{44}-10^{47} erg/s
  energy extending to ~ 1MeV

  “fireball scenario” to explain radiative dissipation and cooling phases

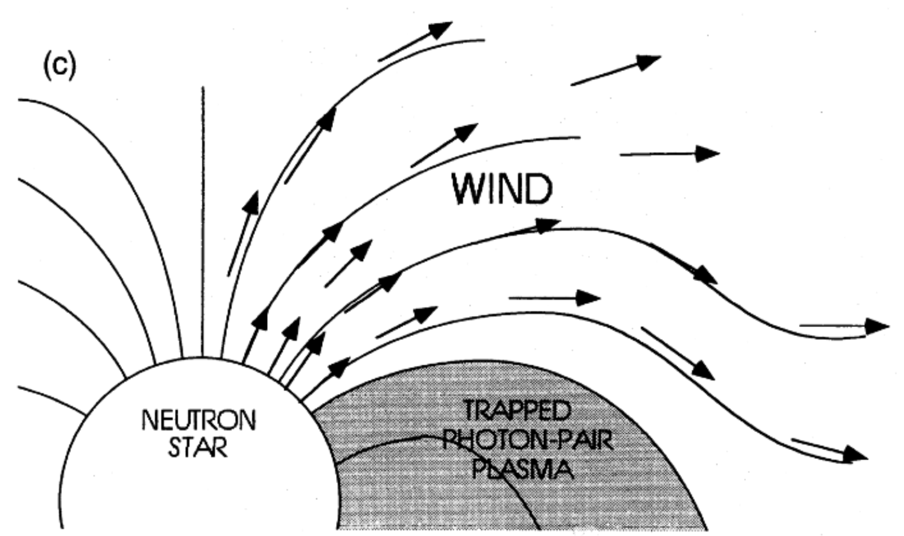

Figure 1. (c) Not all the energy can be contained by the magnetosphere at radius R_{ν}, unless the total energy released is a very small fraction of the dipole magnetic energy of the star. As a result, the pressure of the photon-pair plasma drives a wind from the magnetosphere. This probably occurred in the 1979 March 5 event, but probably not in most ordinary SGR events.

Thompson & Duncan (1995)

Quantum Electrodynamics in Strong Magnetic Fields

pair creation

(a)

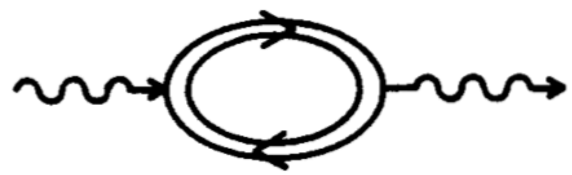

vacuum polarization

(b)

photon splitting

(c)

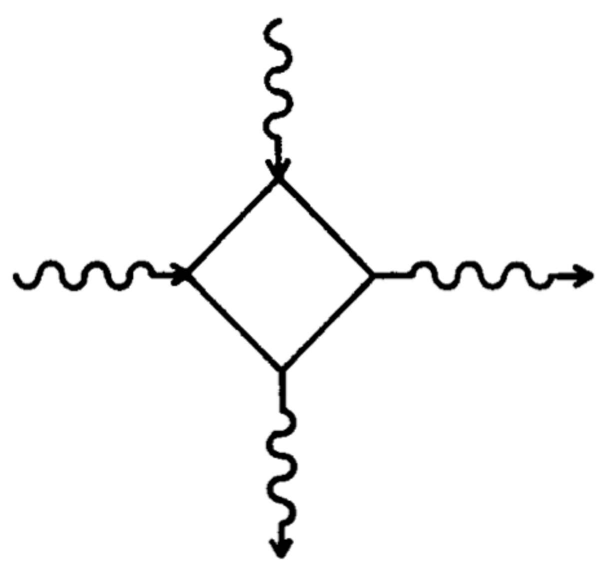

photon scattering

(d)

From Meszaros 1992

$$B_{\rm cr} = m_e^2 c^3/(e\hbar)$$

$$\approx 4.41 \times 10^{13} \text{ Gauss}$$

Vacuum Polarization

- Photons are expected to be polarized in two linear normal modes in the presence of strong magnetic field.
- | | mode (O-mode): photon's electric field vector parallel to the plane containing **B** and **k**
- ⊥ mode (X-mode): photon's electric field vector being normal to the plane containing **B** and **k**

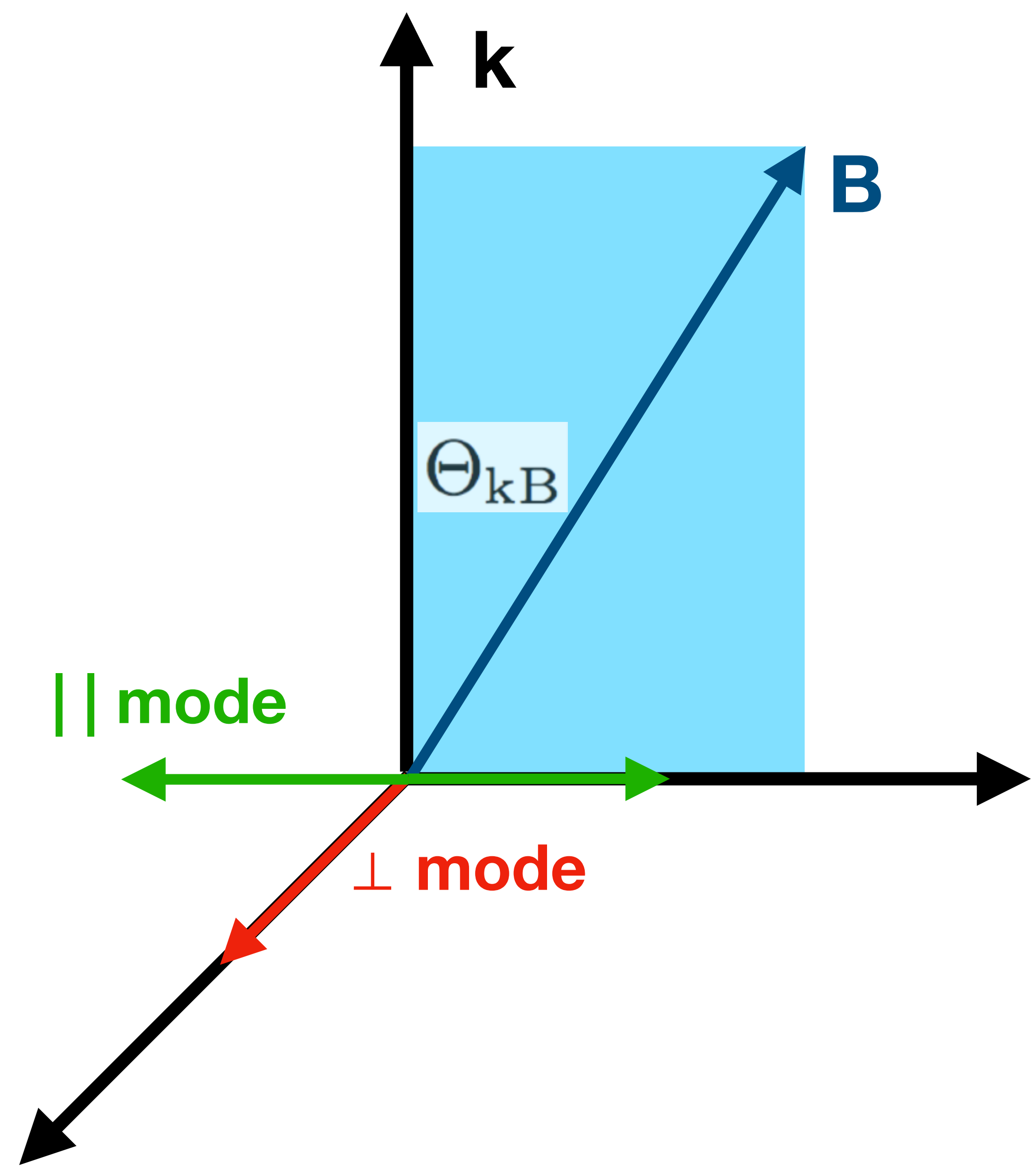

Magnetic Pair Creation

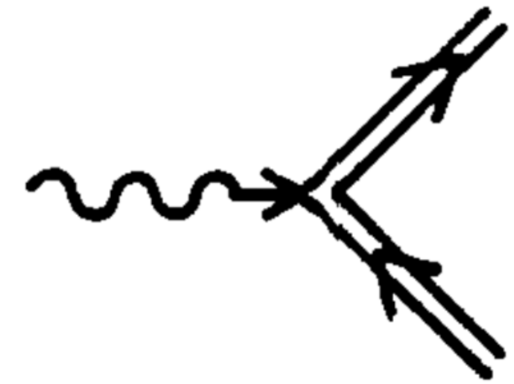

- $\gamma + B \longrightarrow e^+ + e^-$ occurs in strong magnetic fields $B \sim B_{cr} = 4.413 \times 10^{13}$ G
- has a threshold of $2m_ec^2/\sin\Theta_{\rm kB}$ for $\parallel$ mode, and a factor of

  $1 + \sqrt{1+2B}$ higher for $\perp$ mode.

- attenuation coefficients are polarization dependent $(\perp, \parallel)$
- the attenuation coefficient:

$$\mathcal{R}^{\rm pp}_{\parallel,\perp} = \frac{\alpha_{\rm f}}{\lambda_c} B \sin\Theta_{\rm kB}\, \mathcal{F}_{\parallel,\perp}(\varepsilon_\perp,\, B) \ , \quad \varepsilon_\perp = \varepsilon \sin\Theta_{\rm kB}$$

Magnetic Pair Creation

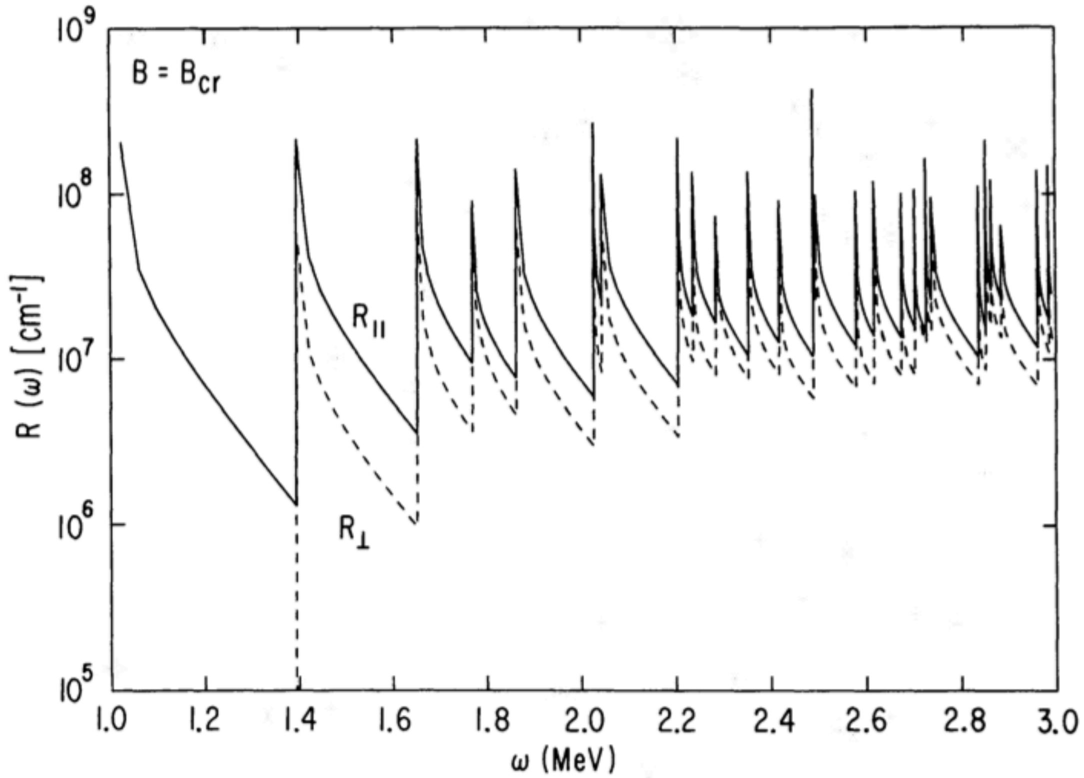

FIG. 2a

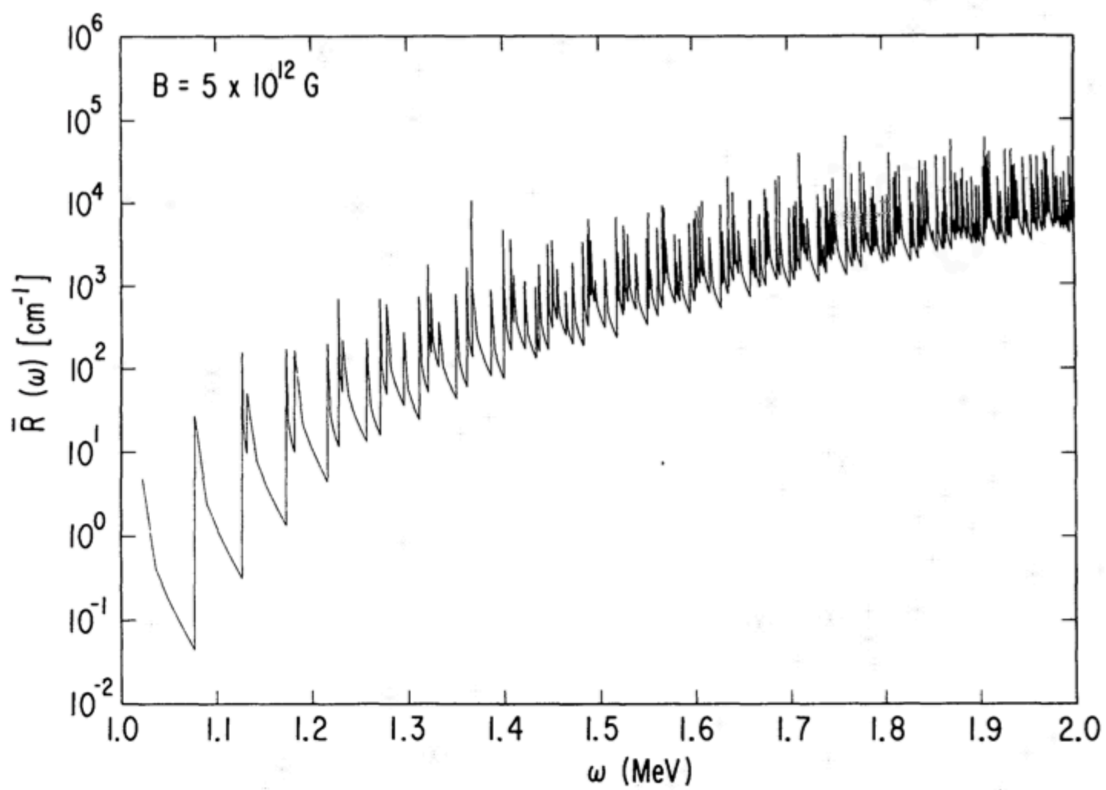

FIG. 2b

$$\mathcal{R}^{\rm pp}_{\|,\perp} = \frac{\alpha_{\rm f}}{\lambda\!\!\!^{-}_c} B \sin\Theta_{\rm kB} \mathcal{F}_{\|,\perp}(\varepsilon_\perp, B) ,$$

$$\varepsilon_\perp = \varepsilon \sin\Theta_{\rm kB}$$

From Daugherty & Harding 1983

Magnetic Photon Splitting

- $\gamma + B \longrightarrow \gamma + \gamma$ occurs in strong magnetic fields B
- has no energy threshold

- attenuation is polarization dependent
- three splitting modes are allowed by CP symmetry:

$$\perp \rightarrow \| \, \| \,, \quad \| \rightarrow \perp \| \,, \text{ and } \perp \rightarrow \perp \perp$$

- only one of them is kinematically allowed in the weakly dispersive regime (Adler's selection rule):

$$\perp \rightarrow \| \, \|$$

may not hold in plasma loaded magnetospheres

Magnetic Photon Splitting

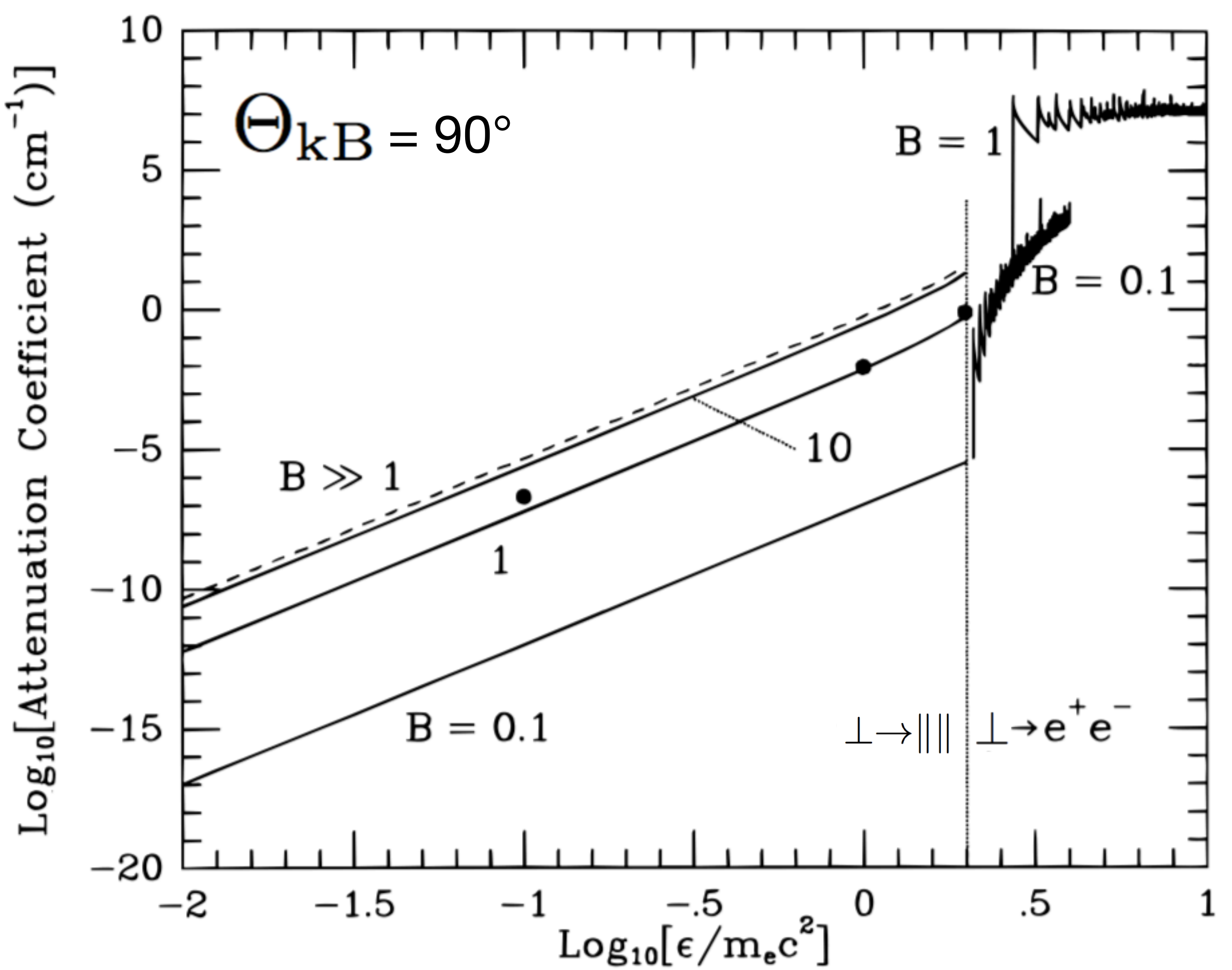

photo splitting coefficient as functions of photon energies with different field strength. Figure from Baring & Harding (1997)

- attenuation coefficients:

$$\mathcal{R}^{\rm sp}_{\perp\to\parallel\parallel} = \frac{\alpha_{\rm f}^3}{60\pi^2\lambda\!\!\!^{-}_c}\,\varepsilon^5\,B^6\,\mathcal{M}_1^2\,\sin^6\Theta_{\rm kB}$$

$$= \frac{1}{2}\,\mathcal{R}^{\rm sp}_{\parallel\to\perp\parallel}$$

$$\mathcal{R}^{\rm sp}_{\perp\to\perp\perp} = \frac{\alpha_{\rm f}^3}{60\pi^2\lambda\!\!\!^{-}_c}\,\varepsilon^5\,B^6\,\mathcal{M}_2^2\,\sin^6\Theta_{\rm kB}$$

- M_1 and M_2 serve as reaction amplitude coefficients

Photon Opacity in NS Magnetosphere

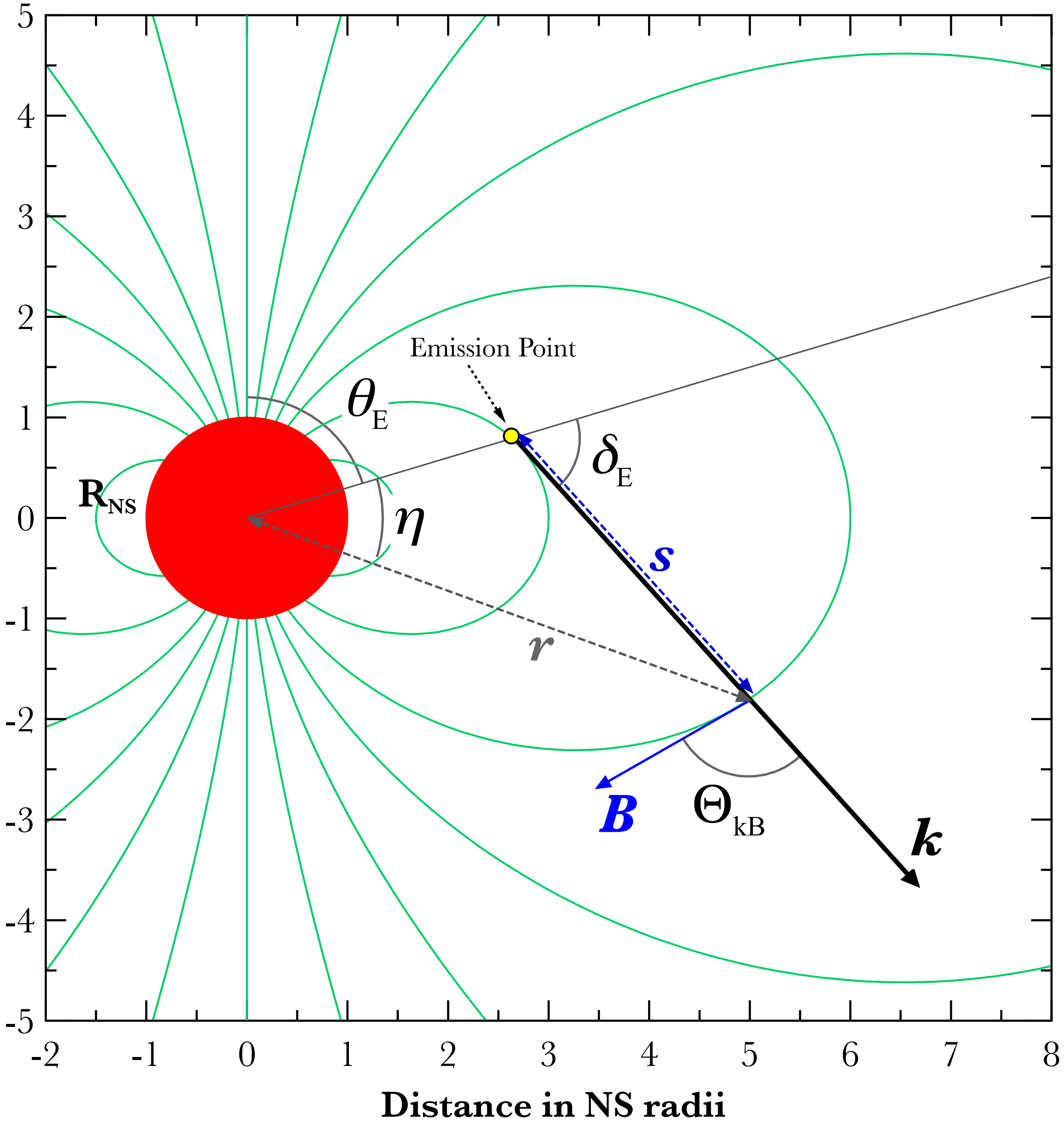

$$\tau(l) = \int_0^l \mathcal{R}\, ds$$

$$\mathcal{R}(\varepsilon, B, \Theta_{kB})$$

- Flat / curved spacetime
- Assume vacuum dipole field
- Photons are generally emitted parallel to the local magnetic field line or make small angle to it (resonant inverse Compton scattering)

Photon Opacity in NS Magnetosphere

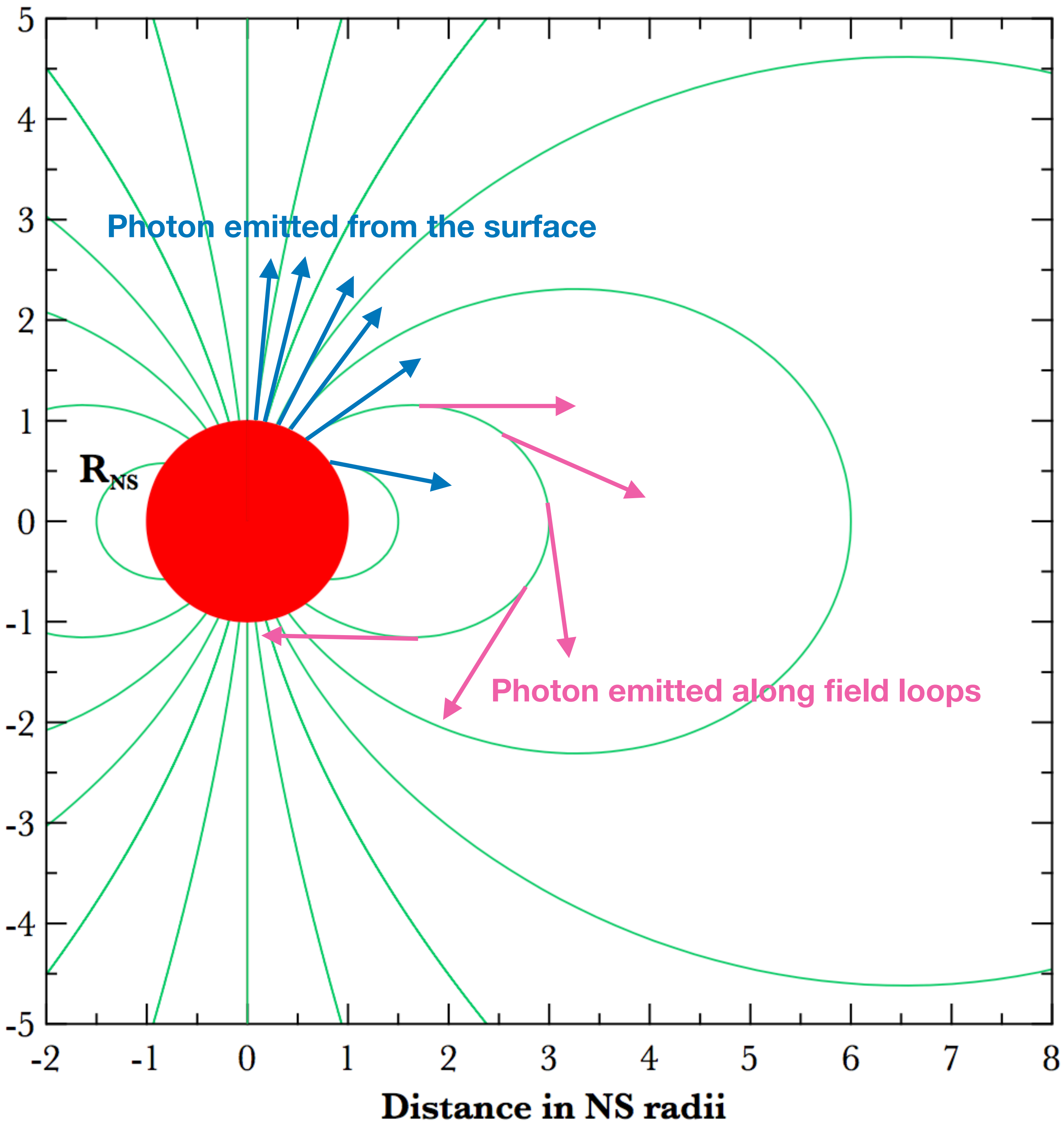

- Photons are emitted from star surface
- Photons are emitted along field loops (applicable to models)

Attenuation Length & Escape energy of Photon Splitting

escape energy

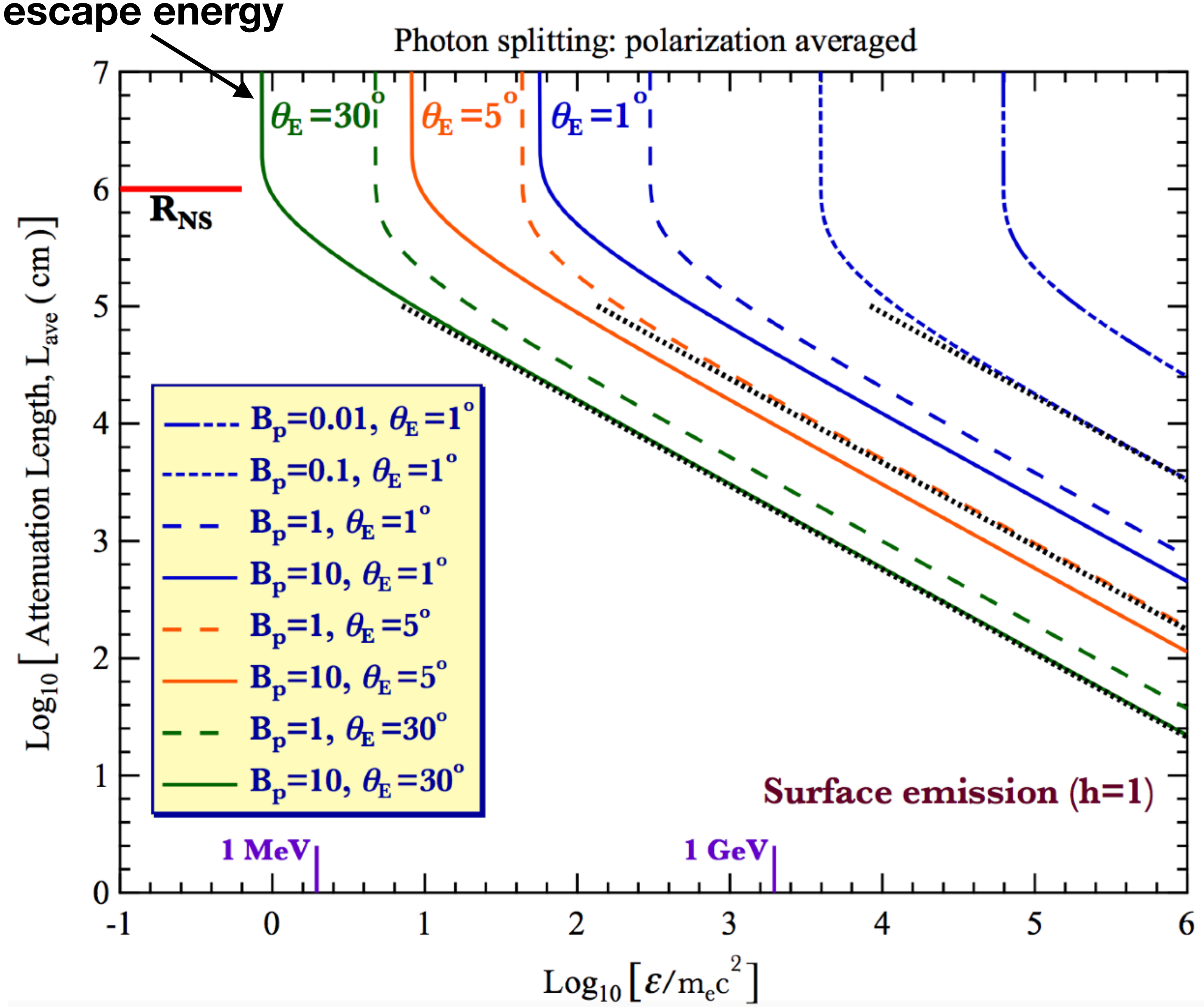

- The attenuation length L is defined to be the path length over which the optical depth equals unity (tau = 1)
- analytic approximation for the low altitude emission (black dotted line)
- The vertical asymptotic divergences define the escape energy
- Below these energies the magnetosphere is transparent to photon splitting

Escape Energy

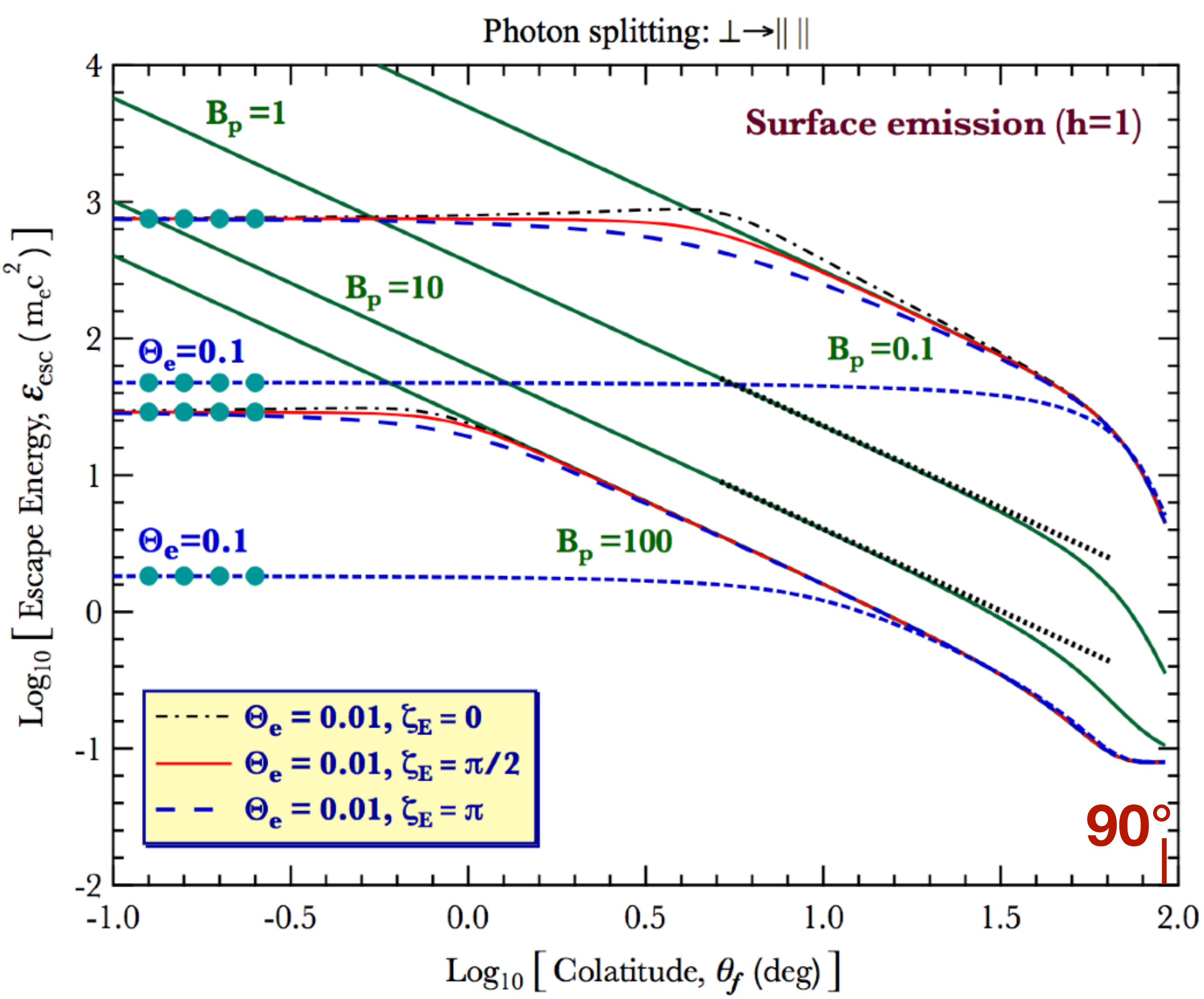

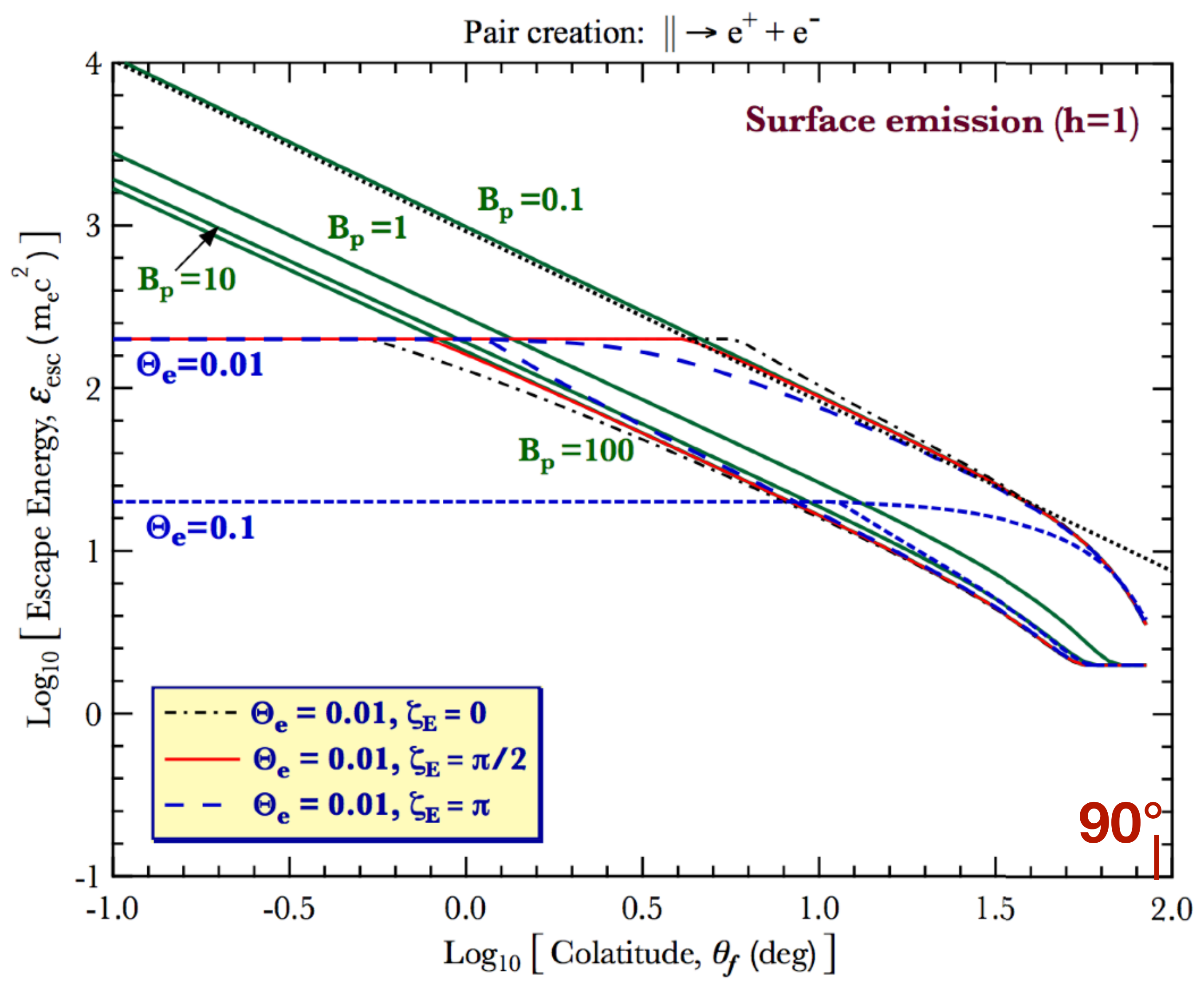

- Escape energies for light emitted from the surface as functions of emitting colatitude

- Green curves: photons emitted parallel to local field lines; red/blue curves: make small angel to field lines

- Bp < 1: pair creation dominates the attenuation; Bp >1 photon splitting dominates.

Photon Opacity in NS Magnetosphere

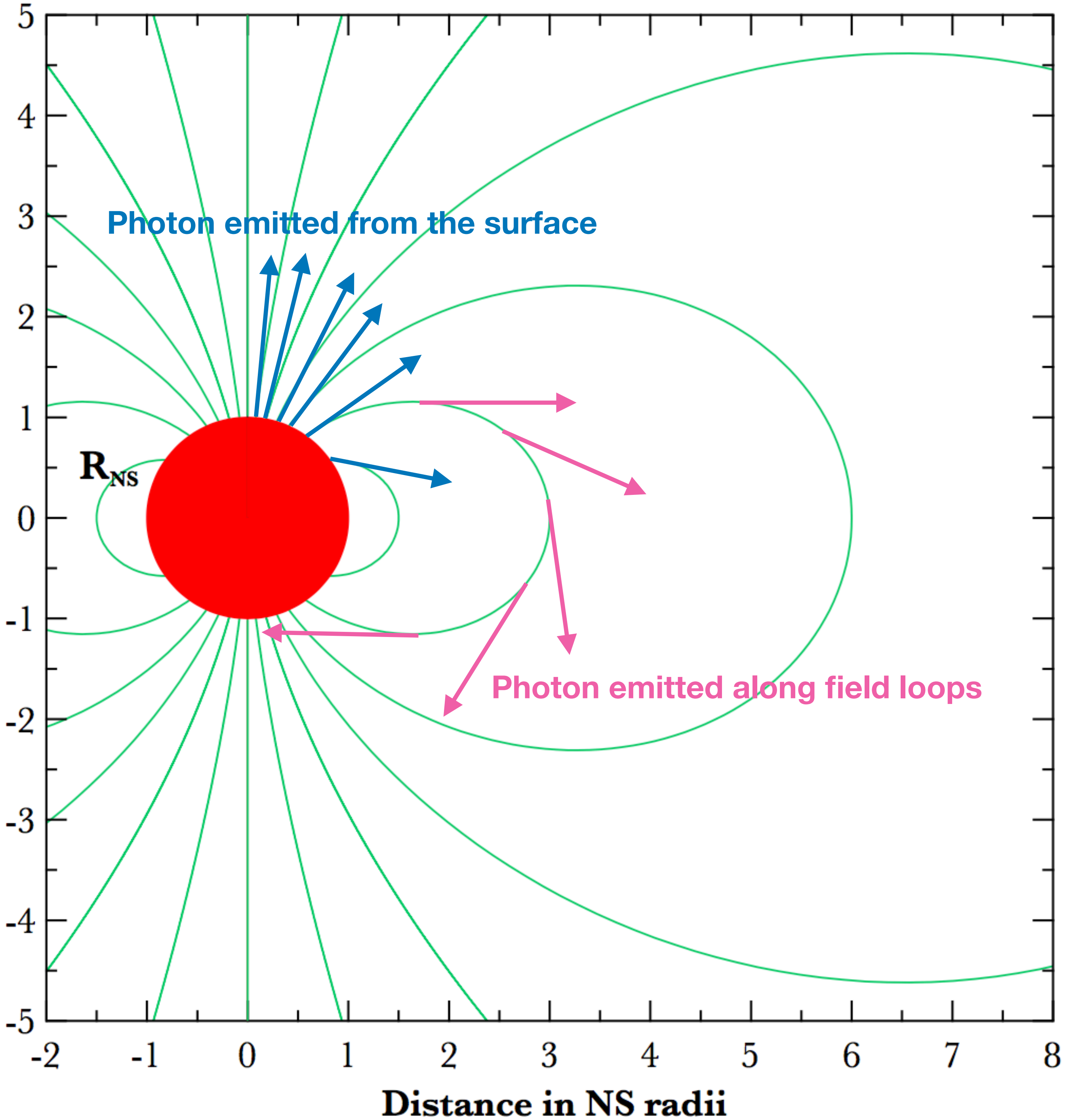

- Photons are emitted from star surface
- Photons are emitted along field loops (applicable to models)

Escape Energy (photon splitting)

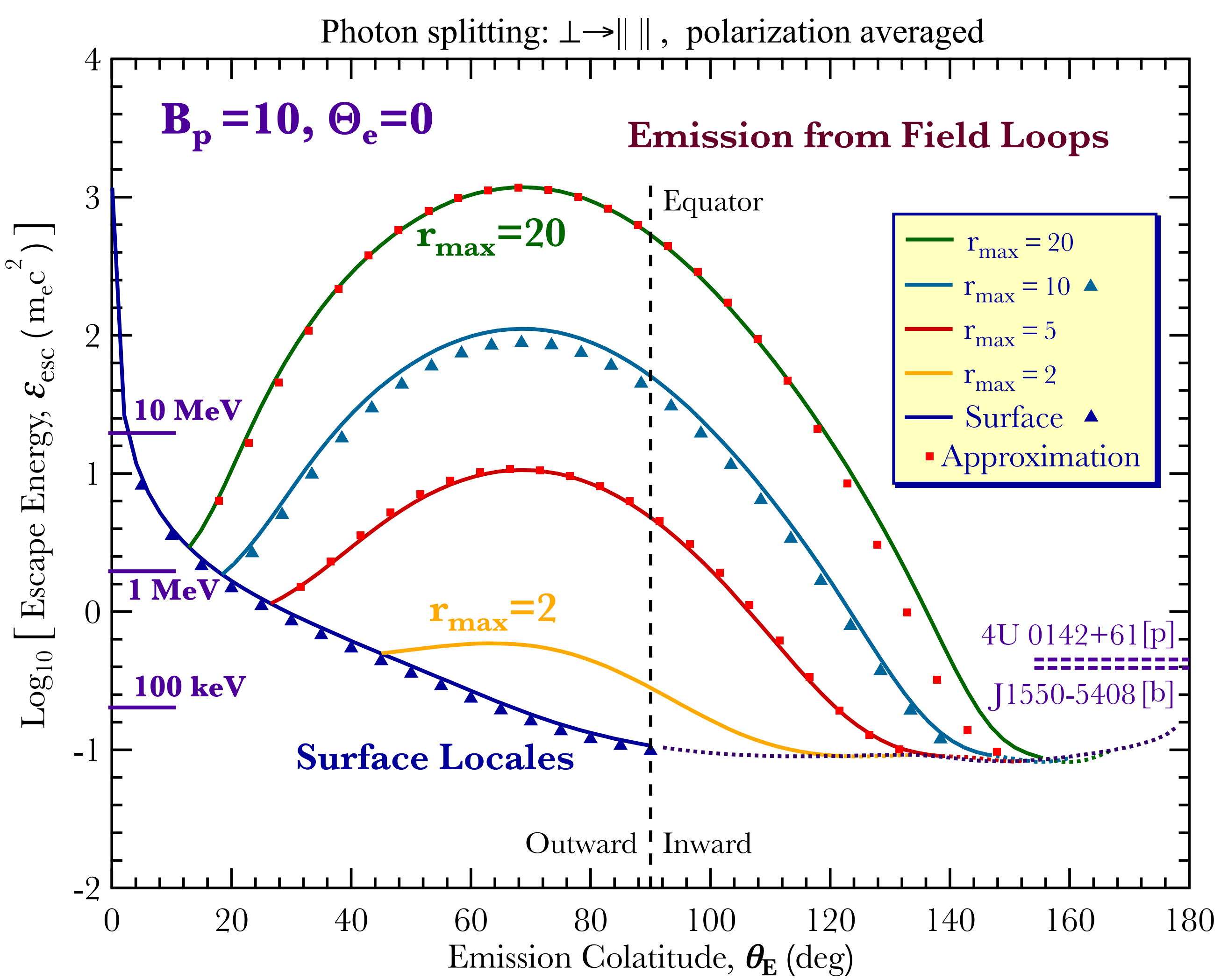

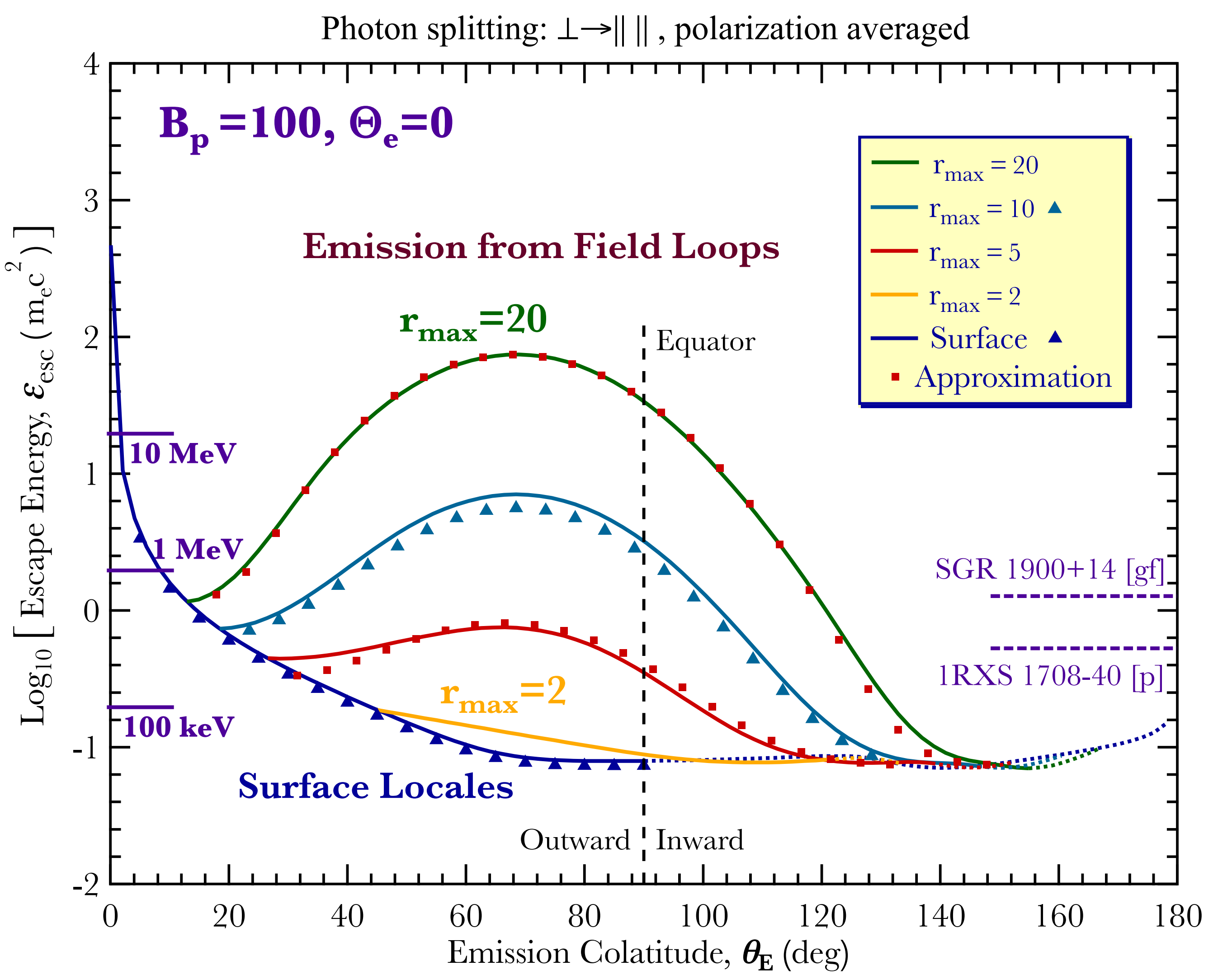

- triangles represent polarization averaged cases
- red dots represent an empirical approximation for loop emission
- dotted curves represent the photons are shadowed by the star, i.e., they impact the surface if not attenuated.

General Relativistic Opacity Construction

$$\omega = \frac{\varepsilon}{\sqrt{1-\Psi}} \quad , \quad \Psi = \frac{r_s}{r} \equiv \frac{2GM}{c^2 r}$$

$$\boldsymbol{B}_{\mathrm{GR}} = 3\frac{B_p \Psi^3}{r_s^3}\left\{\xi_r(\Psi)\,\cos\theta\,\hat{r} + \xi_\theta(\Psi)\,\sin\theta\,\hat{\theta}\right\}$$

$$\xi_r(x) = -\frac{1}{x^3}\left[\log_e(1-x) + x + \frac{x^2}{2}\right]$$

$$\xi_\theta(x) = \frac{1}{x^3\sqrt{1-x}}\left[(1-x)\,\log_e(1-x) + x - \frac{x^2}{2}\right]$$

$$\theta(\Psi) \equiv \theta_{\mathrm{E}} + \Delta\theta = \theta_{\mathrm{E}} \pm \int_{\Psi}^{\Psi_{\mathrm{E}}} \frac{d\Psi_r}{\sqrt{\Psi_b^2 - \Psi_r^2(1-\Psi_r)}}$$

$$\sin\Theta_{\mathrm{kB}} = \frac{\sqrt{\Psi_b^2 - \Psi^2(1-\Psi)} - \Psi\sqrt{1-\Psi}\,\xi(\Psi)\,\cot\theta}{\Psi_b\sqrt{1+[\xi(\Psi)]^2\cot^2\theta}}$$

- GR influences: gravitational redshift, the deformation of the dipole field, curved photon trajectories
- GR are expected to increase the opacities in most parameter regimes

$$\tau(\Psi) = r_s \int_{\Psi}^{\Psi_{\mathrm{E}}} \frac{\mathcal{R}(\omega,\,\sin\Theta_{\mathrm{kB}},|\boldsymbol{B}_{\mathrm{GR}}|)\,\Psi_b\,d\Psi_r}{\Psi_r^2\sqrt{(1-\Psi_r)\,\{\Psi_b^2 - \Psi_r^2(1-\Psi_r)\}}}$$

Escape Energy (splitting +pairs)

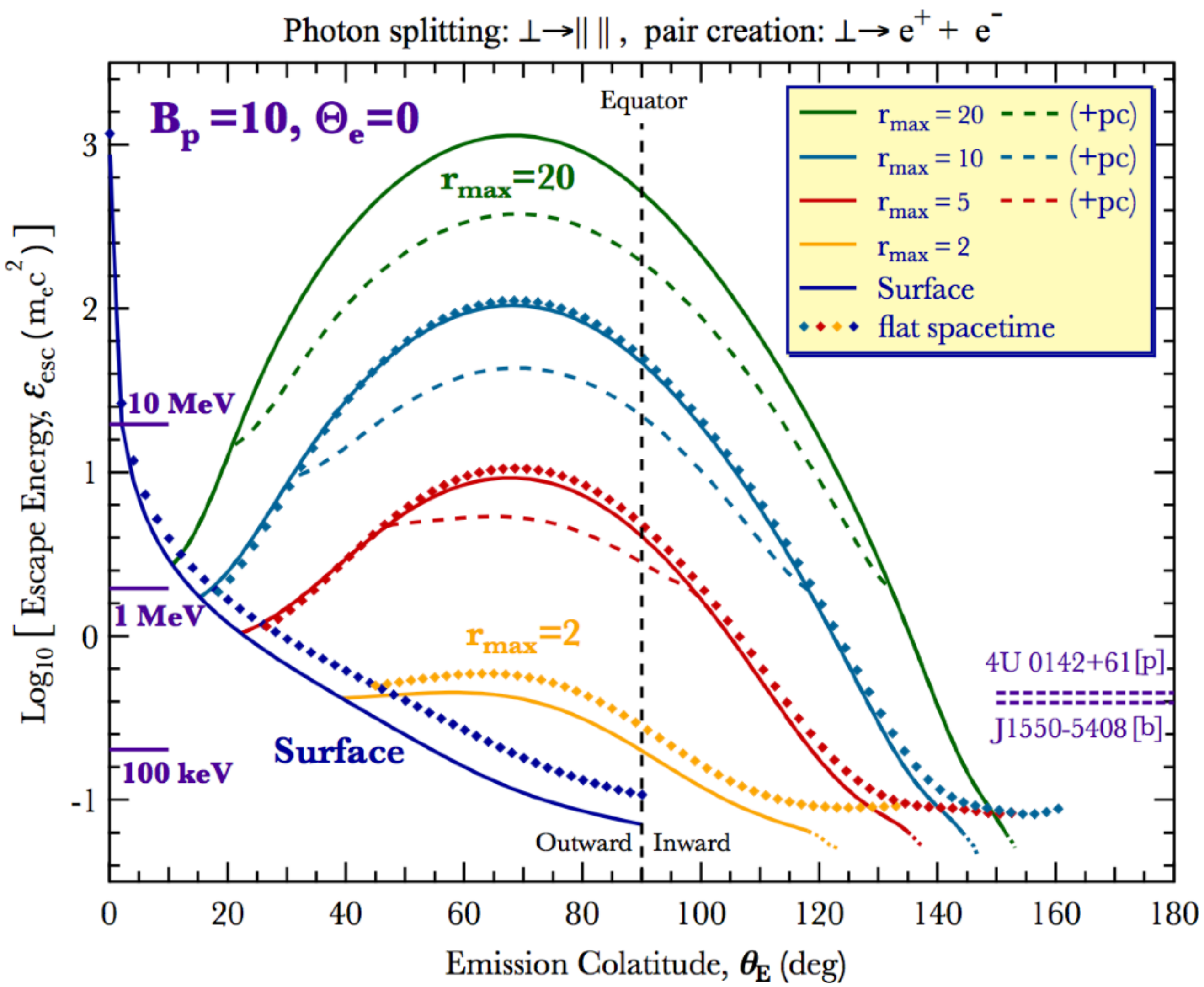

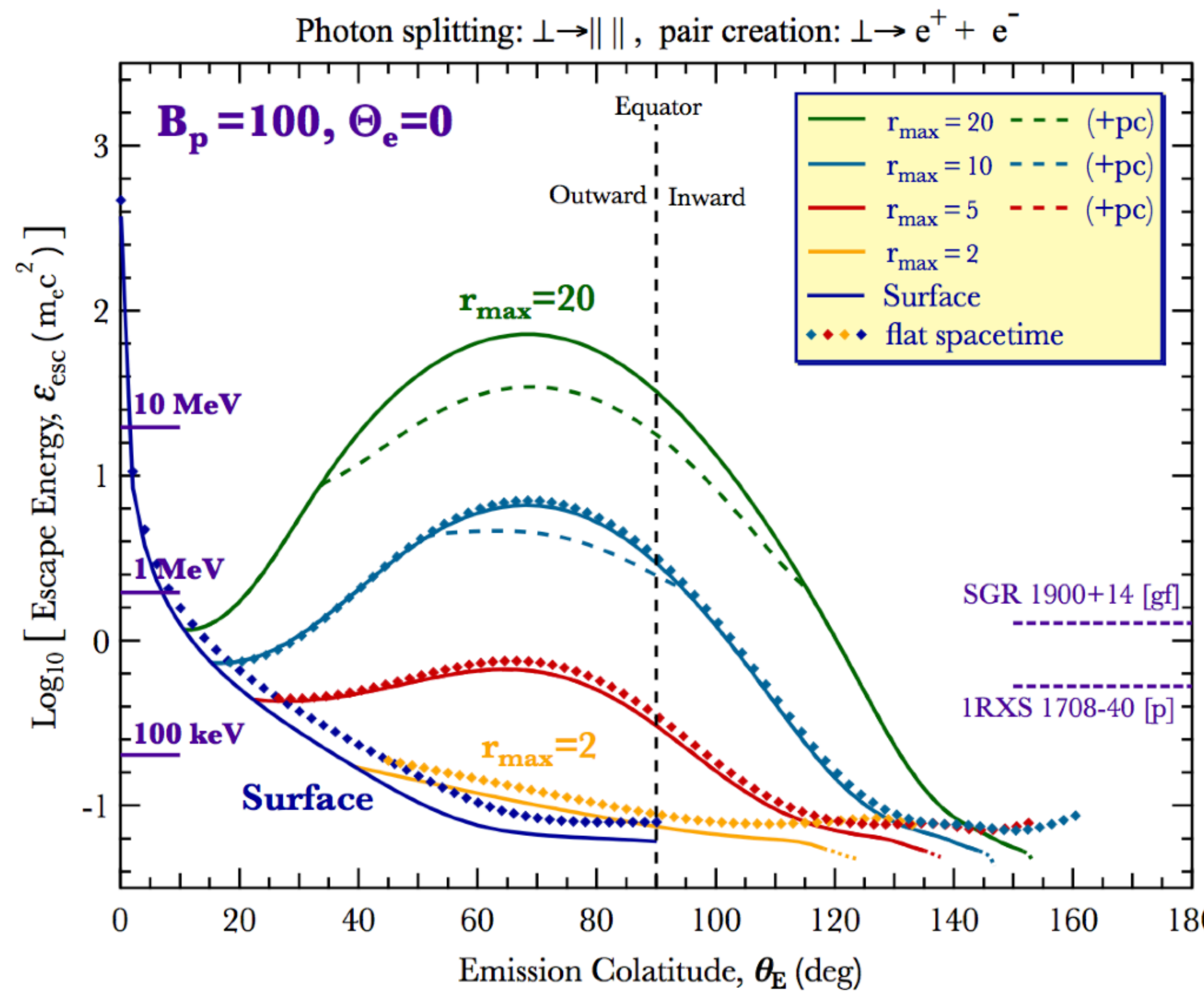

- solid curves represent results for curved spacetime
- dashed curves display a combination of pair creation and photon splitting
- GR effect is important for low attitude emission

Splittosphere

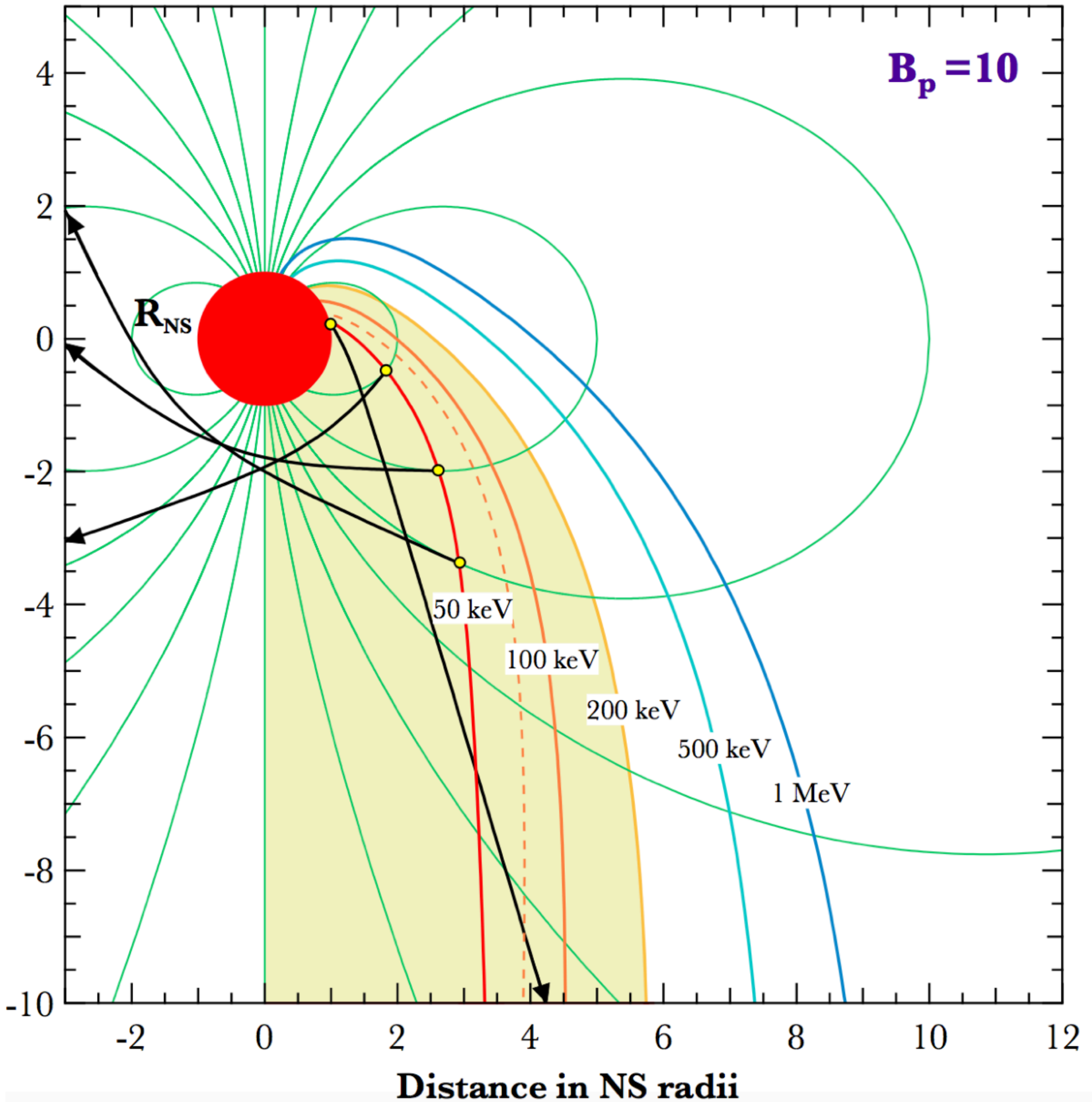

- Colored contours represent the lowest possible emission altitude for transparency at a given colatitude
- Photon trajectories are plotted for selected emission points on the 50 keV contour
- dashed orange contour is a flat spacetime version of the 100 keV case

RICS cutoff energy and ⊥ mode photon splitting escape energy

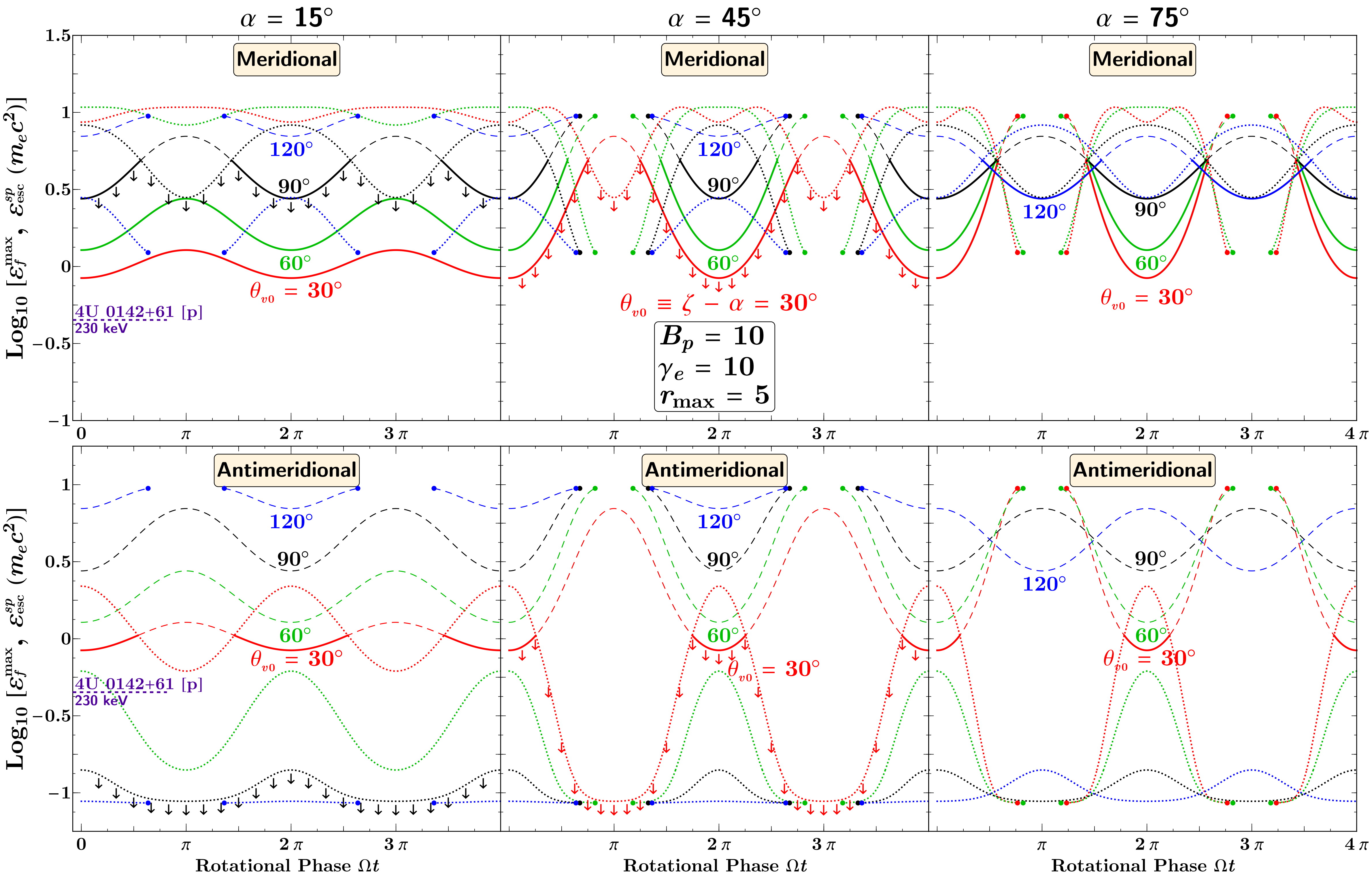

- Resonate inverse Compton scattering maximum cut off energies: solid/dashed curves
- Escape energies : dotted curves

Summary

- Calculation of the opacities of pair creation and photon splitting provides upper bound to the visible energies

- provides constraints to the altitude of the hard X-ray emission from magnetars: for Bp = 10, the persistent and flaring emission must be produced with r_max > 2; for Bp =100, the emission must be produced with r_max > 5

- strongly-polarized signatures are expected for future missions (AMEGO and e-ASTROGAM): determine which photon splitting mode operates in the magnetospheres of magnetars; phase-resolved spectropolarimetry can help determine geometric parameters like the inclination angle α

Backup Slides

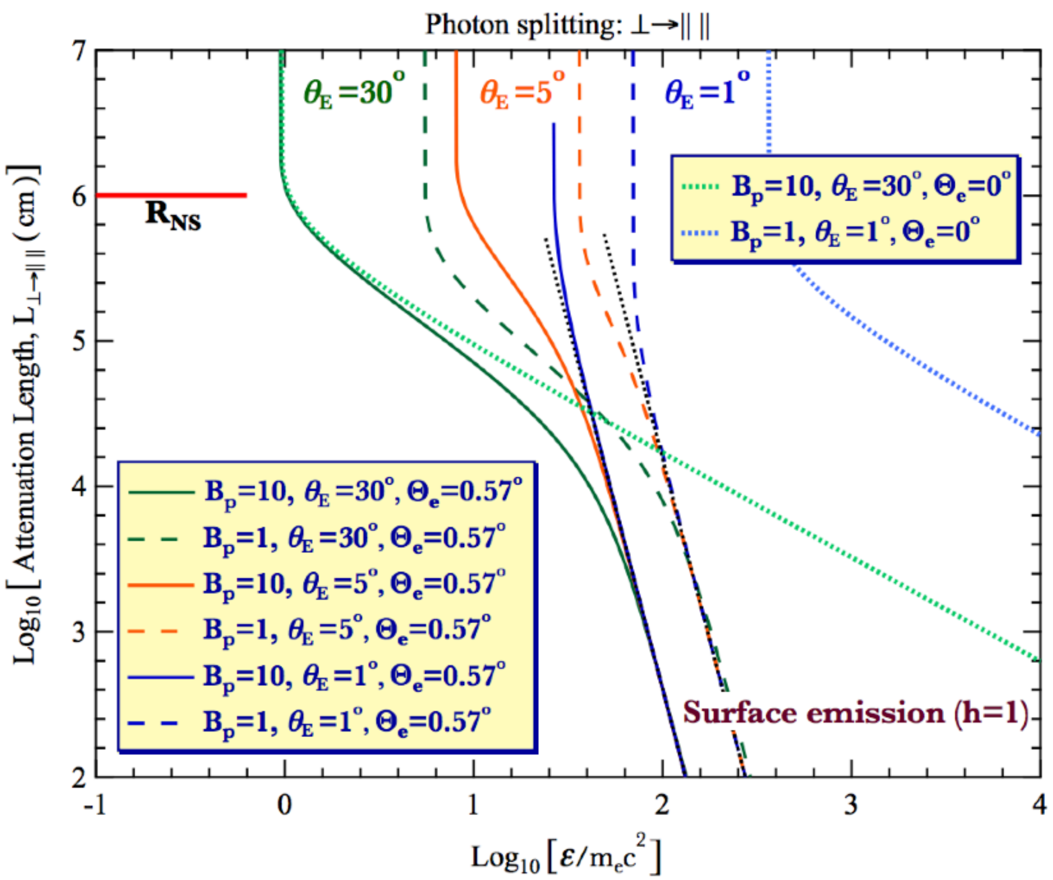

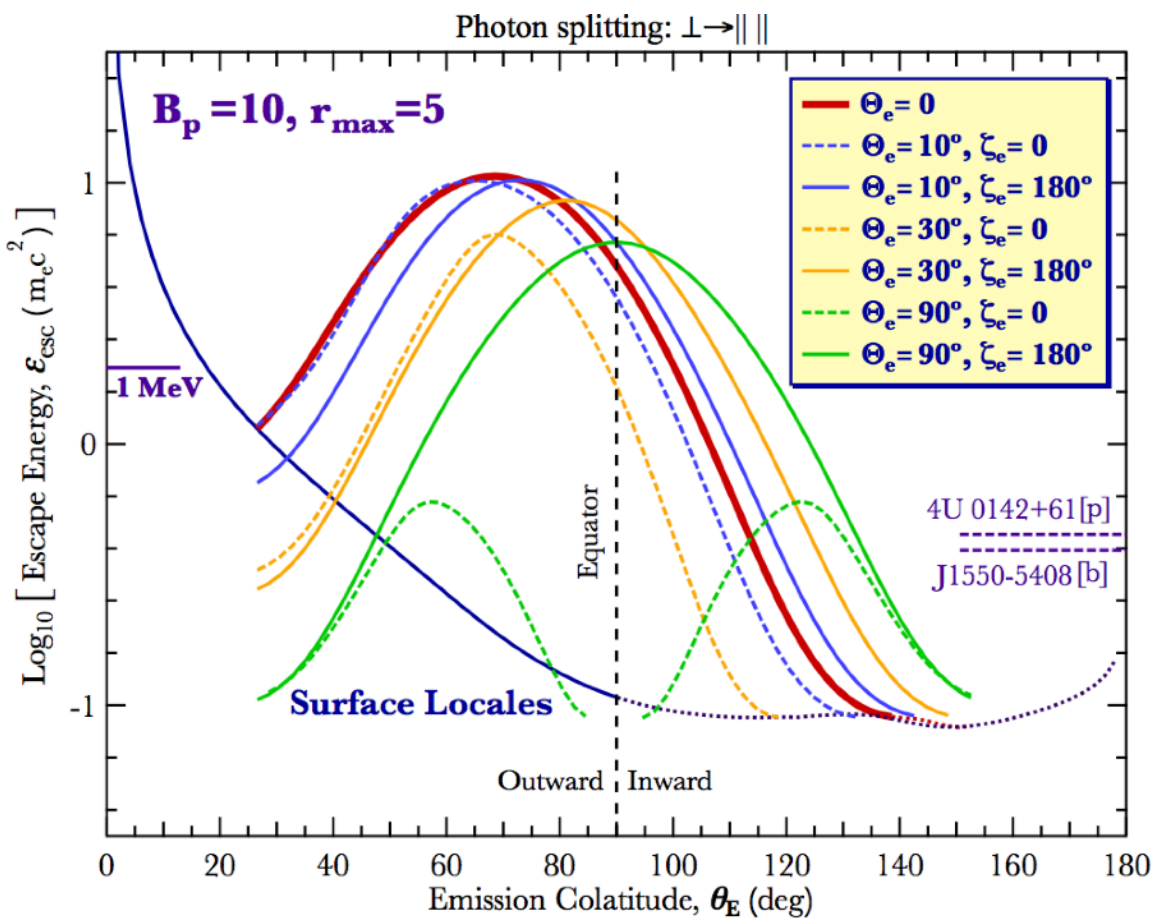

Wadiasingh et al. 2019

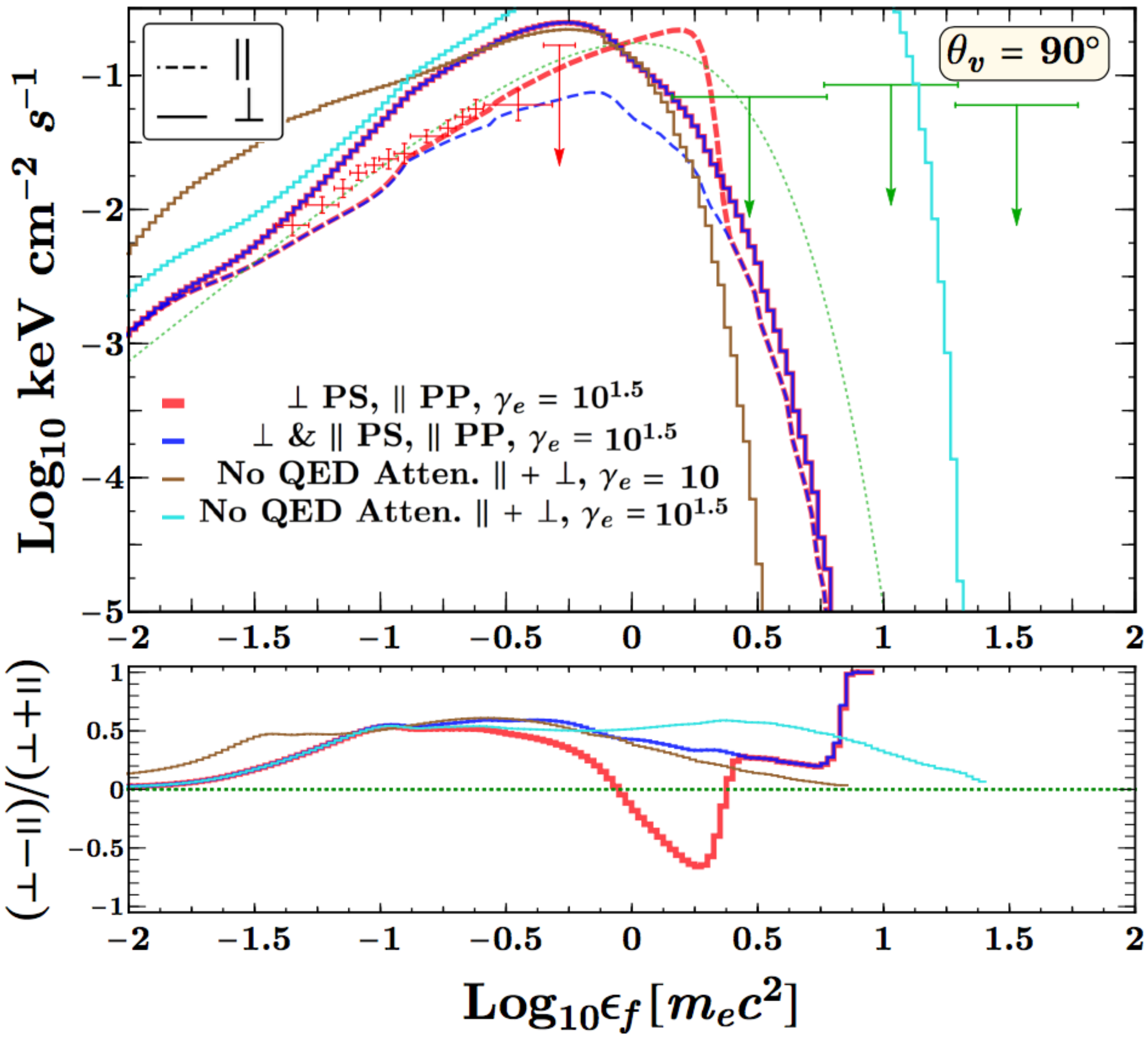

Spin-phase resolved model RICS spectra and signed polarization for different electron Lorentz and propagation influences.

- Spin-phase resolved model RICS spectra of a generic magnetar (at arbitrary normalization) overlaid on phase-averaged data for 4U 0412+61 along with a PL with exponential cutoff at 350 keV in dotted green.
- Without inclusion of QED opacities, the cutoff is kinematically attained and exponential in character
- Future missions (AMEGO and e-ASTROGAM) are expected to see these differences

Persistent Emission

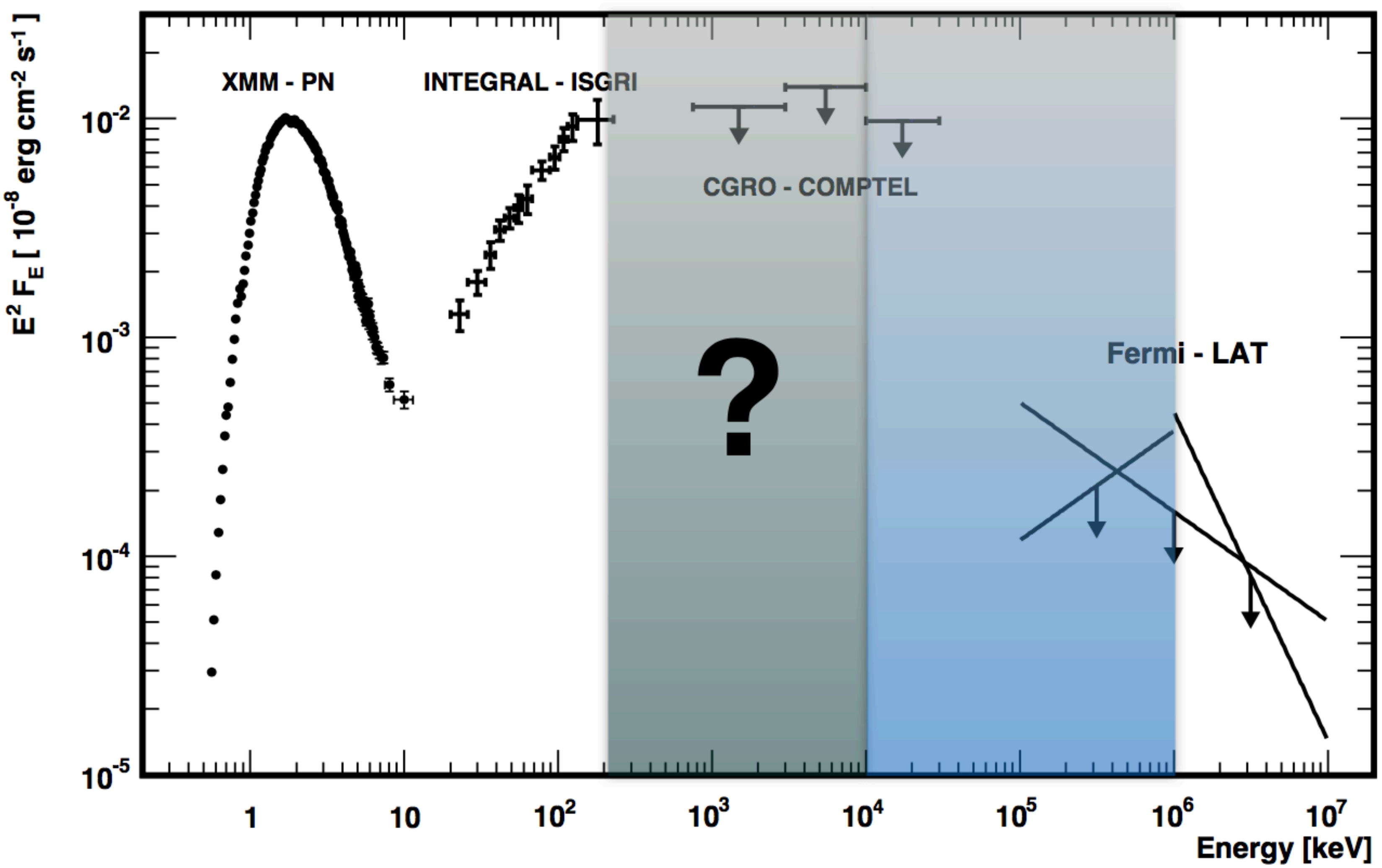

Total spectra of 4U 0142+61 as measured with different instruments. Figure adapted from Abdo et al.(2010)

- In quiescent state, magnetars emit quasi-thermal X-ray kT~0.5 keV
- soft X-ray luminosities exceed spin down energy loss
- hard X-ray (>10 keV) spectra : flat power law with a typical index ~1-2
- hard X-ray mechanism : resonant inverse Compton scattering

Recurrent Short Bursts

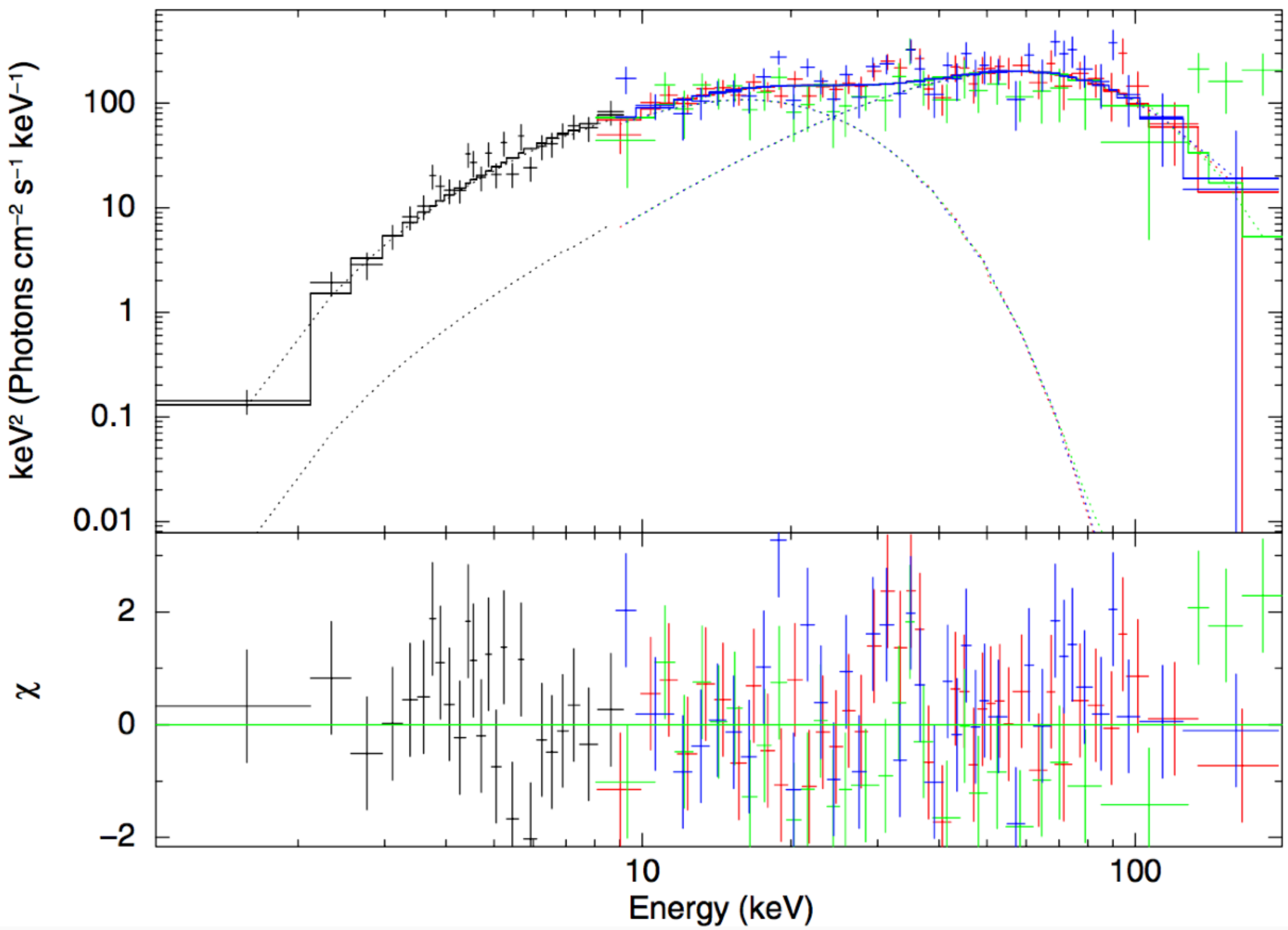

Spectrum of the magnetar SGR J1550-5418 burst detected on 2009 January 22 fitted by a two blackbody model.
Figure from Lin et al. (2012)

- often occur in storms lasting a month or more
- peak luminosity ~10^{37}-10^{43} erg/s, last ~ 0.1s
- spectra can be fit by comptonized model or bremsstrahlung model (~30 keV) or a two-blackbody model

Giant Flare

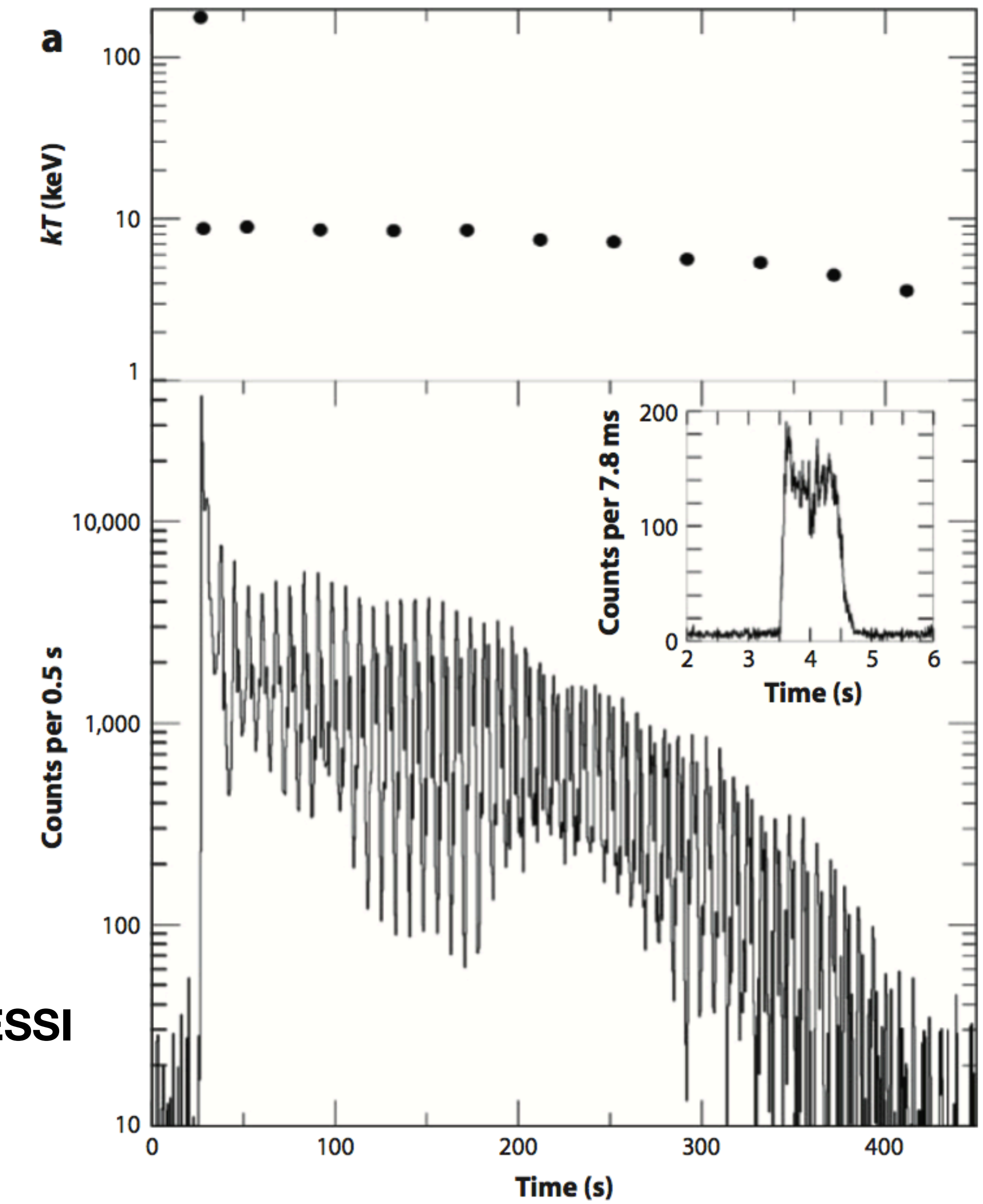

from the RHESSI satellite

The Blackbody temperature and the 20–100-keV time history for the 2004 SGR 1806–20 giant flare. Figure from Victoria M. Kaspi et al. (2017), adapted from Hurley et al. (2005)

- a hard spike lasting~0.2s, peak luminosity~10^{44}-10^{47} erg/s
- followed by an energetic tail persisting for several minutes
- only three giant flares have been recorded
- "fireball scenario" to explain radiative dissipation and cooling phases

Photon Opacity in NS Magnetosphere

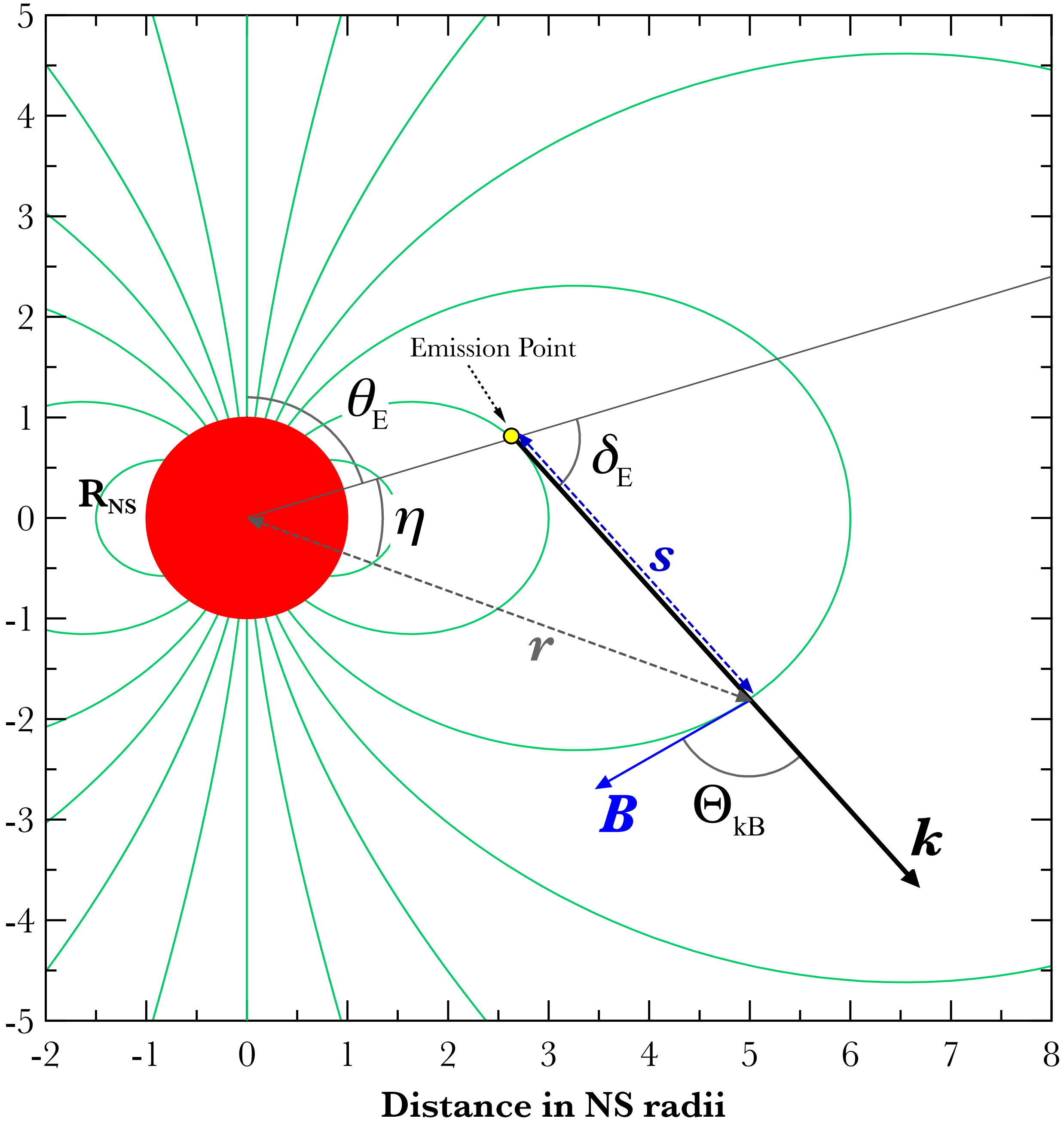

$$\tau(l) = \int_0^l \mathcal{R}\, ds$$

- Flat / curved spacetime

- Dipole field

$$\boldsymbol{B} = \frac{B_p R_{NS}^3}{2r^3}\left(2\cos\theta\,\hat{\boldsymbol{r}} + \sin\theta\,\hat{\boldsymbol{\theta}}\right)$$

- Photons are generally emitted parallel to the local magnetic field line or make small angle to it (resonant inverse Compton scattering)

Emission Mechanism

Thompson & Duncan (1995)

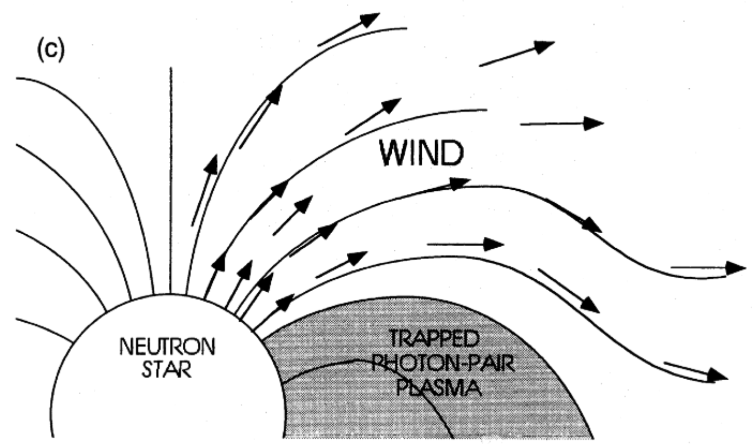

Figure 1. (c) Not all the energy can be contained by the magnetosphere at radius R_p, unless the total energy released is a very small fraction of the dipole magnetic energy of the star. As a result, the pressure of the photon-pair plasma drives a wind from the magnetosphere. This probably occurred in the 1979 March 5 event, but probably not in most ordinary SGR events.

Wadiasingh et al. (2018)

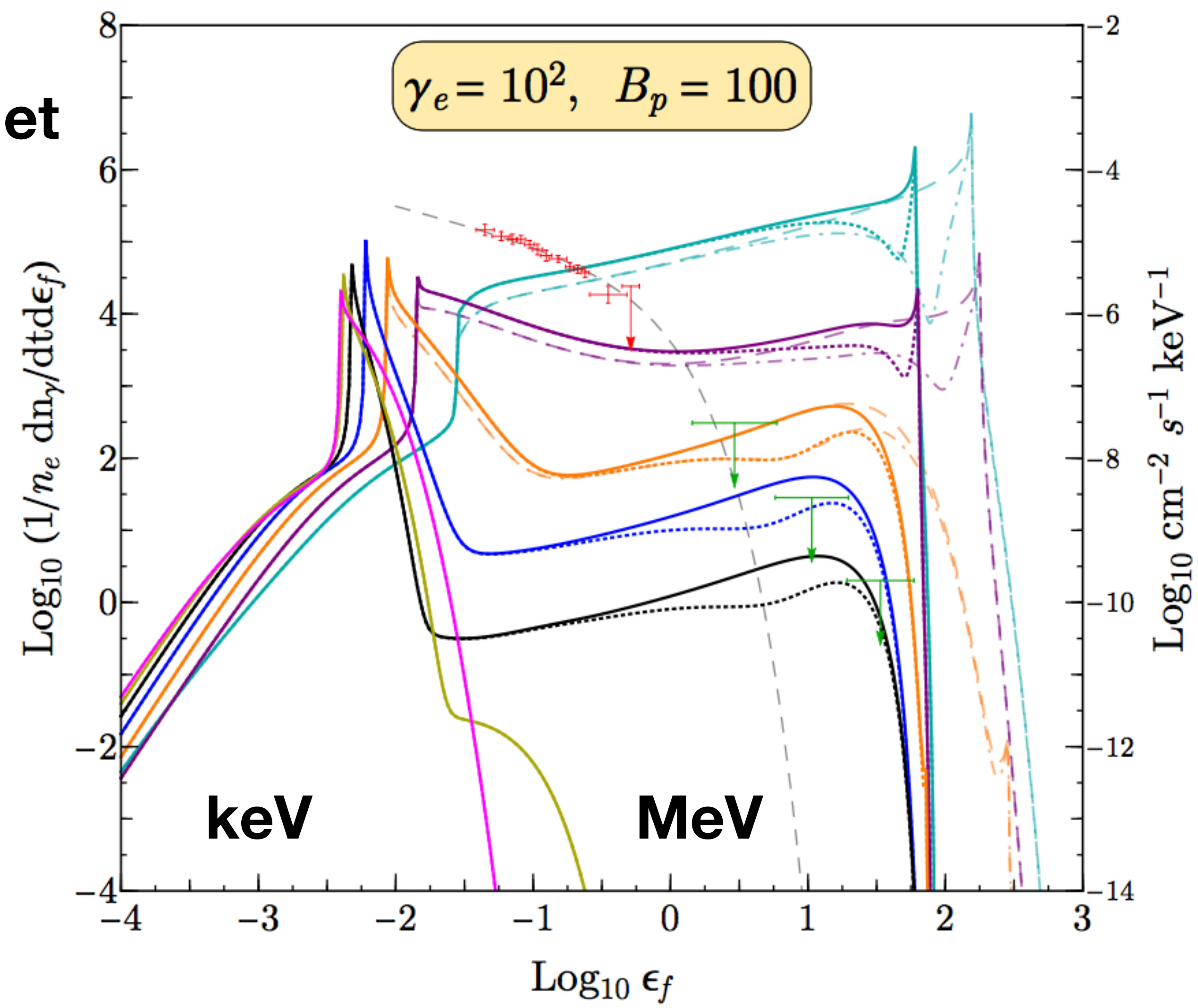

- Burst emission: fireball scenario
- non-thermal soft X-ray persistent emission: resonant cyclotron scattering near the atmosphere
- non-thermal hard X-ray persistent emission: resonant Compton upscattering